PENSOFT
SENCKENBERG world of biodiversity
Leibniz Association

Molecular phylogenetic and morphological studies reveal increased species diversity in the millipede genus *Skleroprotopus* Attems, 1901 in China (Julida: Mongoliulidae)

Rong Chen[1], Yi Zhao[1,2], Sergei Golovatch[3], Wei-Xin Liu[1]

1 *College of Plant Protection, South China Agricultural University, 483 Wushan Road, Guangzhou 510642, China*
2 *Guangdong Academy of Forestry, 233 Guangshan 1st Road, Guangzhou 510520, China*
3 *Institute for Problems of Ecology and Evolution, Russian Academy of Sciences, Leninsky pr. 33, Moscow 119071, Russia*

https://zoobank.org/927B910A-4F53-4BBA-B9A7-D60B1EF4733E

Corresponding author: Wei-Xin Liu (da2000wei@163.com)

Received 11 September 2024
Accepted 21 October 2024
Published 18 December 2024

Academic Editors Andy Sombke, Klaus-Dieter Klass

Citation: Chen R, Zhao Y, Golovatch S, Liu W-X (2024) Molecular phylogenetic and morphological studies reveal increased species diversity in the millipede genus *Skleroprotopus* Attems, 1901 in China (Julida: Mongoliulidae). Arthropod Systematics & Phylogeny 82: 659–691. https://doi.org/10.3897/asp.82.e136751

Abstract

A taxonomic study of the genus *Skleroprotopus* Attems, 1901 from nine provinces in China was conducted utilizing morphological comparisons and molecular phylogenetic analyses. The results reveal thirteen new species, i.e. *Skleroprotopus yutiantianae* **sp. nov.**, *S. tiankeng* **sp. nov.**, *S. megistus* **sp. nov.**, *S. penglai* **sp. nov.**, *S. longissimus* **sp. nov.**, *S. genjudi* **sp. nov.**, *S. laiyuanensis* **sp. nov.**, *S. longiflagellatus* **sp. nov.**, *S. change* **sp. nov.**, *S. ampullaceus* **sp. nov.**, *S. incisodentatus* **sp. nov.**, *S. multistriatus* **sp. nov.**, and *S. conicus* **sp. nov.** This significantly enriches the diversity of *Skleroprotopus* in China, bringing it to a total of 18 species. With the exception of *S. yutiantianae* **sp. nov.**, all these species were collected in caves. In terms of their degree of adaptation to the cave environment, the latter six species are presumed troglophiles, while the others are likely troglobites. DNA-barcoding based on the COI mitochondrial gene is documented for the first time in this genus. The specific *p*-distances between *Skleroprotopus* species range from 6.6–17.0%, while intraspecific *p*-distances are only 0.2–1.4%. Additionally, the morphological features of male leg-pair 1, the penis and leg-pair 7 are also discussed.

Keywords

barcoding, cave, diversity, new species, phylogeny

1. Introduction

The Mongoliulidae Pocock, 1903 is a small family of julidan millipedes that presently encompass about 36 species in six genera. These range from the Russian Far East in the north, throughout Korea and Japan, to the northern mainland of China in the south (Enghoff et al. 2017; Mikhaljova 2019). Among the six genera recognized, four are monospecific: *Ikahoiulus leucosoma* Takakuwa, 1941 (Japan), *Koiulus interruptus* Enghoff, Jensen and Mikhaljova, 2017 (Russian Far East), *Uenoiulus notabilis* Murakami, 1971 (Japan), and *Ussuriiulus pilifer* Golo-

vatch, 1980 (Russian Far East). The genus *Kopidoiulus* Attems, 1909 comprises seven species, one of which, *K. continentalis* Golovatch, 1979, lives both in the Russian Far East and northeastern China (e.g. Enghoff et al. 2017).

Skleroprotopus Attems, 1901 is the largest and most widespread genus of Mongoliulidae. Currently, it contains 25 species, primarily distributed in the eastern Palearctic, being confined to the Russian Far East, Korea, Japan, and northern China (Mikhaljova 2019; Mikhaljova et al. 2024). The main characteristics of this genus can be found in Mikhaljova (2004): male prementum swollen, prominent, soft; male leg-pair 1 strongly enlarged and modified into claspers; male leg pair 7 with a coxal process and a telopodite with variable podomere numbers; anterior gonopod with a coxal process and a flagellum at base; posterior gonopod with two branches.

So far, only five species of *Skleroprotopus* are known in China: *S. confucius* Attems, 1901 (Zhangjiahou City, Hebei Province), *S. laticoxalis* Takakuwa, 1942 (Shenyang City, Liaoning Province), *S. membranipedalis* Zhang, 1985 (Beijing), *S. securifer* Mikhaljova, 2024 (Xiaowutai Mt., Hebei Province), *S. serratus* Takakuwa, 1949 (Taiyuan City, Shanxi Province) (Golovatch and Liu 2020). Of them, *S. membranipedalis* is the only species recognized as a true cave-dweller, with completely unpigmented eyes and only reported from Shihua Dong and Cloud Water Dong caves (Vagalinski et al. 2018). Additionally, there are only six gene sequences related to Mongoliulidae species that can be found on NCBI (Enghoff et al. 2011; Jiang et al. 2023), which makes the study of the phylogeny of this family considerably more difficult.

Following a prolonged period of field surveys and material collections, a number of *Skleroprotopus* species have been discovered in southern China. In this study, we describe 13 new species from nine provinces in China, of which 12 species are found in caves. Additionally, we present the molecular data of four gene fragments for the genus. Integrating DNA sequences not only provides an effective method for species identification, but also offers valuable data for further studies on the phylogeny of Mongoliulidae.

2. Materials and methods

2.1. Morphological analysis

The material for this study was collected by hand and preserved in 95% ethanol. The types are deposited in the Zoological Collection of the South China Agricultural University (SCAU), Guangzhou, Guangdong Province, China. The pictures of the living animals were taken with a Canon EOS 40D camera (Tokyo, Japan). Detailed examination of characters and dissections were performed using a Leica S8 APO stereo microscope (Wetzlar, Germany). Photographs of the specimens were taken with a Keyence VHX-5000 digital microscope (Osaka, Japan) and edited using Adobe Photoshop CS6. The terminology used in the text follows that of Mikhaljova and Korsós (2003) and Enghoff et al. (2017).

2.2. Molecular analyses

2.2.1. DNA extraction and sequencing

Genomic DNA was extracted from muscle tissue using a Qiagen DNeasy Blood and Tissue kit following the manufacturer's extraction protocol. Partial sequences of two mitochondrial genes (COI and 16S) and two nuclear genes (18S and 28S) were amplified using the degenerate primers HCO2198-JJ/LCO1490-JJ (Folmer et al. 1994), 16Sar/16Sb (Simon et al. 1994; Edgecombe et al. 2002), 18S-5'/18S-b5.0 (Shull et al. 2001) and 28SH/28SL (Muraji and Tachikawa 2000), respectively (Table S1). PCR amplification was performed using a T100™ thermal cycler (Bio-Rad, Singapore) with a final reaction volume of 25 µl. Sanger sequencing results were edited and assembled using the SeqMan module of Lasergene, and the identities confirmed with BLAST searches (https://blast.ncbi.nlm.nih.gov/Blast.cgi) (Altschul et al. 1997).

In addition, sequences from four species of Julida were downloaded from GenBank, along with sequences obtained from two non-Julida species (consisting of a Spirostreptida and a Spirobolida) for use as outgroups. All species analyzed, voucher numbers and GenBank accession numbers are listed in Table 1.

2.2.2. Sequence alignment and phylogenetic analyses

All molecular analyses were conducted on the PhyloSuite v.1.2.3 platform (Xiang et al. 2023). Protein-coding gene sequences (COI) were aligned using codon-aware MACSE software, while the more variable sequences (16S, 18S, 28S) were aligned using MAFFT. The best partitioning scheme and evolutionary models for analyses were selected using PartitionFinder2 with all-algorithm and AICc criterion.

Maximum likelihood (ML) phylogenies were inferred using IQ-TREE v. 1.6.8 for 1000 standard bootstraps. Bayesian Inference (BI) phylogenies were implemented by MrBayes 3.2.6 under the partition model (2 parallel runs, 2000000 generations), in which the initial 25% sampled data were discarded as burn-in. The resulting phylogenetic trees were visualized and edited with Figtree v.1.4.4.

2.2.3. Distance and species delimitations

The distance analysis involved 21 COI sequences (19 new sequences and 2 from GenBank). Codon positions included were 1st+2nd+3rd. All positions containing 'N's were removed for each sequence pair (pairwise deletion). Uncorrected *p*-distances of COI markers were calculated using MEGA X (Kumar et al. 2018).

Table 1. List of the species used for molecular phylogenetic analyses and their relevant information. *: new sequence; /: missing.

Taxon	Voucher number	COI	16S	18S	28S
Skleroprotopus change sp. nov. *	SCAUZY11	PQ246765	PQ282231	PQ238331	PQ238313
Skleroprotopus conicus sp. nov. *	SCAUZY04	PQ246778	PQ282226	PQ238326	PQ238308
Skleroprotopus conicus sp. nov. *	SCAUZY23	PQ246779	PQ282238	PQ238338	PQ238319
Skleroprotopus genjudi sp. nov. *	SCAUZY03	PQ246767	PQ282225	PQ238325	PQ238307
Skleroprotopus genjudi sp. nov. *	SCAUZY25	PQ246768	PQ282240	PQ238340	PQ238321
Skleroprotopus longissimus sp. nov. *	SCAUZY06	PQ246769	PQ282228	PQ238328	PQ238310
Skleroprotopus laiyuanensis sp. nov. *	SCAUZY07	PQ246772	PQ282229	PQ238329	PQ238311
Skleroprotopus laiyuanensis sp. nov. *	SCAUZY21	PQ246773	PQ282237	PQ238337	PQ238318
Skleroprotopus longiflagellatus sp. nov. *	SCAUZY29	PQ246774	/	PQ238342	PQ238323
Skleroprotopus incisodentatus sp. nov. *	SCAUZY15	PQ246770	PQ282234	PQ238334	PQ238316
Skleroprotopus incisodentatus sp. nov. *	SCAUZY18	PQ246771	PQ282236	PQ238336	PQ238317
Skleroprotopus megistus sp. nov. *	SCAUZY16	PQ246775	PQ282235	PQ238335	/
Skleroprotopus membranipedalis	JXK001	OP104940	OP106395	OP106387	OP106413
Skleroprotopus multistriatus sp. nov. *	SCAUZY24	PQ246776	PQ282239	PQ238339	PQ238320
Skleroprotopus penglai sp.nov. *	SCAUZY28	PQ246777	/	PQ238341	PQ238322
Skleroprotopus ampullaceus sp. nov. *	SCAUZY14	PQ246766	PQ282233	PQ238333	PQ238315
Skleroprotopus tiankeng sp. nov. *	SCAUZY05	PQ246780	PQ282227	PQ238327	PQ238309
Skleroprotopus yutiantianae sp. nov. *	SCAUZY13	PQ246781	PQ282232	PQ238332	PQ238314
Outgroup Mongoliulidae, Julida					
Kopidoiulus continentalis	ZMUC100957	/	JF320991	/	JF321046
Outgroup Nemasomatidae, Julida					
Nemasoma varicorne	ZMUC101184	JN619379	JF320976	/	JF321031
Outgroup Julidae, Julida					
Ophyiulus pilosus	ZMUC200176	/	JF320969	/	JF321024
Ophyiulus pilosus	ZSMMYR00154	HQ966125			
Ophyiulus pilosus	KMPFM133			EU685194	/
Outgroup Blaniulidae, Julida					
Proteroiulus fuscus	ZMUC101185	JN619376	JF320973	/	JF321028
Proteroiulus fuscus	MCZDNA100171			AF173236	
Outgroup Spirobolidae, Spirobolida					
Spirobolus sp. *	SCAUZY02	PQ246782	PQ282224	PQ238324	PQ238306
Outgroup Pericambalidae, Spirostreptida					
Pericambala sinica *	SCAUZY09	PQ246783	PQ282230	PQ238330	PQ238312

Both Automatic Barcode Gap Discovery (ABGD) (https://bioinfo.mnhn.fr/abi/public/abgd/abgdweb.html) and Bayesian implementation of Poisson Tree Processes (bPTP) (https://species.h-its.org/ptp) were used to separately delimitate taxa for COI and 16S. All of the parameters follow default settings, while the relative gap width was set at 1.0.

2.2.4. Distribution mapping

The distribution map was created using ArcGIS 10.8.1 (Fischer and Geris 2009) by entering the latitude and longitude of each species collection site.

3. Results

3.1. Phylogenetic tree description

The final aligned dataset included 24 sequences, each with 642 bp of COI, 580 bp of 16S rRNA, 609 bp of 18S rRNA and 529 bp of 28S rRNA. The combined analysis after these exclusions consisted of 2360 positions.

As the phylogenetic tree estimated by both ML and BI analyses revealed essentially identical topologies, here we only present the ML tree (Fig. 1). It is evident that the order Julida is a monophyletic group, while the monophyly of the family Mongoliulidae (only two genera included here) is not strongly supported (PP = 0.81, BS = 66%). The monophyly of the genus *Skleroprotopus* was strongly supported by 1.0 PP for BI, but a little weaker, at 82% BS, for ML. Within the ingroup species, the topology may imply that it can be divided into two clades (PP = 1.0, BS = 82%), with one containing *S. membranipedalis* + *S. tiankeng* **sp. nov.** + *S. megistus* **sp. nov.** + *S. yutiantianae* **sp. nov.**, and the remaining ten species in the other clade. Furthermore, the majority of internal nodes were weakly supported, except for *S. tiankeng* **sp. nov.** and *S. megistus* **sp. nov.**, which are the sister group to each other, with 100% support. In addition to this, strong supports are observed for the sister relationship between *S. incisodentatus* **sp. nov.** and *S. multistriatus* **sp. nov.**, as indicated by PP of 1.0 and BS of 92%; also *S. change* **sp. nov.** and *S. longiflagellatus* **sp. nov.**, as indicated by PP of 1.0 and BS of 99%.

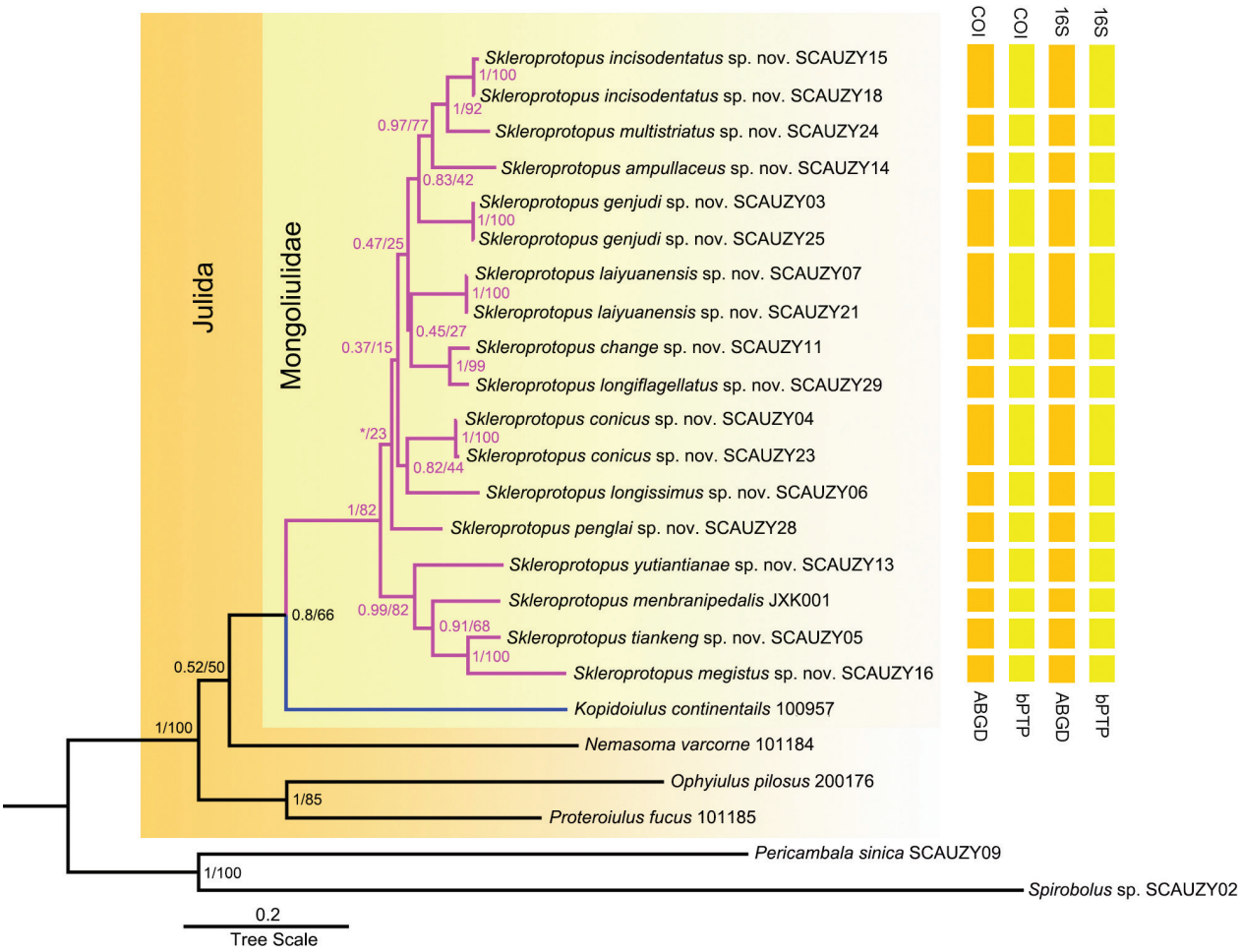

Figure 1. Maximum likelihood phylogenetic tree based on sequences of four gene fragments. Numbers at nodes indicate Bayesian posterior probability (PP) (left side of /) from BI and bootstrap values (BS) from ML. Sidebars indicate species delimitations proposed by ABGD and bPTP approaches.

3.2. Species delimitations and genetic distances

We performed species delimitations for the COI and 16S genes using both ABGD and bPTP analyses. The results from these computer analyses were consistent with the phylogenetic tree, classifying the genus *Skleroprotopus* into 14 operational taxonomic units (OTUs) (Fig. 1). Duplicates from different individuals within the same species were also grouped into the same OTU, and the outgroups were accurately delineated as well.

The number of base differences per site between sequences is shown in Table S2. Uncorrected pairwise distances between *Skleroprotopus* and the three outgroups were found to be generally high, varying between 15.8–27.8%. Amongst the *Skleroprotopus* species concerned in our dataset, the interspecific genetic distances ranged from 6.6% (between *S. change* **sp. nov.** and *S. longiflagellatus* **sp. nov.**) to 17.0% (between *S. yutiantianae* **sp. nov.** and *S. longissimus* **sp. nov.**). The intraspecific divergence was found to range from 0.2–1.4%. Intraspecific distances between different individuals are 0.2% in *S. genjudi* **sp. nov.**, 0.5% in *S. laiyuanensis* **sp. nov.**, 1.1% in *S. conicus* **sp. nov.** and 1.4% in *S. incisodentatus* **sp. nov.**.

3.3. Taxonomy

3.3.1. *Skleroprotopus yutiantianae* sp. nov.

https://zoobank.org/4A7A2586-DE72-4ADE-86E5-368AE6AD5CB8

Figures 3F, 4

Material examined. Holotype male (SCAU), China, Qinghai Province, Xining City, Chengzhong District, Nanshan Park, 36°36′3.78″N 101°46′6.08″E, 2400 m, 18.VIII.2020, Yu Tiantian leg.

Diagnosis. Differs from congeners mostly based on the following combination of characters: (1) leg 1, 6-segmented (Fig. 4D); (2) penis much shorter than coxae 2 (Fig. 4F); (3) coxal process of leg 7 (Fig. 4E) tongue-shaped, about 2× as long as a club-shaped telopodite; (4) anterior gonopod with a very long and narrow coxal process, carrying an irregularly dentate and membranous lobe (Fig. 4I). — In addition, this new species differs from all other species analyzed in a >12.7% uncorrected *p*-distance of the COI barcoding gene.

Figure 2. Pictures of live animals, photos by Prof. Mingyi Tian from SCAU. **A** *Skleroprotopus change* **sp. nov.**; **B** *Skleroprotopus megistus* **sp. nov.**; **C** *Skleroprotopus longissimus* **sp. nov.**; **D** *Skleroprotopus genjudi* **sp. nov.**; **E** *Skleroprotopus tiankeng* **sp. nov.**; **F** *Skleroprotopus laiyuanensis* **sp. nov.**; **G** *Skleroprotopus incisodentatus* **sp. nov.**

Etymology. The specific epithet is honored to Dr. Yu Tiantian (余甜甜) (Kunming Institute of Zoology, Chinese Academy of Sciences), who is the collector; noun in the genitive case.

Description. Length of holotype ca 25.0 mm, 1.6 mm in diameter, body with 53 podous + 1 apodous rings + telson. Coloration in alcohol marbled dark brownish, slightly lighter in anterior 1/3 body (Fig. 3F). Antennae semi-transparent, gradually infuscate from base to end, antennomeres 5 and 6 darkest, frosted violet (Fig. 4C). Eye patches blackish, triangular, arranged in 6 irregular rows, about 35 (left) or 43 (right) ommatidia per eye patch (Fig. 4B). Legs pale yellow.

Head capsule (Fig. 4B) smooth and hairless, vertex bulged, epicranial suture obviously concave. Labral margin with 2+2 supra-labral and 6(7)+6(7) labral setae (Fig. 4A). Antennae (Fig. 4C) medium in length, reaching behind to middle of ring 2 when stretched dorsally. In length, antennomeres 3>2>4>6≈5>1>7. Antennomeres 5 and 6 each with a distal corolla of sensilla basiconica. Antennomere 7 invaginated terminally, sensory cones inconspicuous. Mandibular stipes enlarged, with two nearly equal lobes (Fig. 3F). Gnathochilarium with at least 4

Figure 3. Habitus of some *Skleroprotopus* species in lateral view. **A** *Skleroprotopus penglai* **sp. nov.**; **B** *Skleroprotopus longiflagellatus* **sp. nov.**; **C** *Skleroprotopus tiankeng* **sp. nov.**; **D** *Skleroprotopus ampullaceus* **sp. nov.**; **E** *Skleroprotopus conicus* **sp. nov.**; **F** *Skleroprotopus yutiantianae* **sp. nov.**; **G** *Skleroprotopus multistriatus* **sp. nov.**; **H** *Skleroprotopus change* **sp. nov. Scale bars:** 5.0 mm.

setae on each lamella lingualis (**ll**); prementum (**pr**) long and diamond-shaped, swollen anteriorly (Fig. 4A).

Collum (Fig. 3F) with 6 lower striae laterally, but lowest stria not reaching the anterior margin. Prozona delicately alveolate, metazona laterally with 13–18 longitudinal striae (Fig. 3F). Suture dividing pro- and metazona narrow, a regular comb. Ozopores starting with ring 6, lying anteriorly on lateral sides of metatergites.

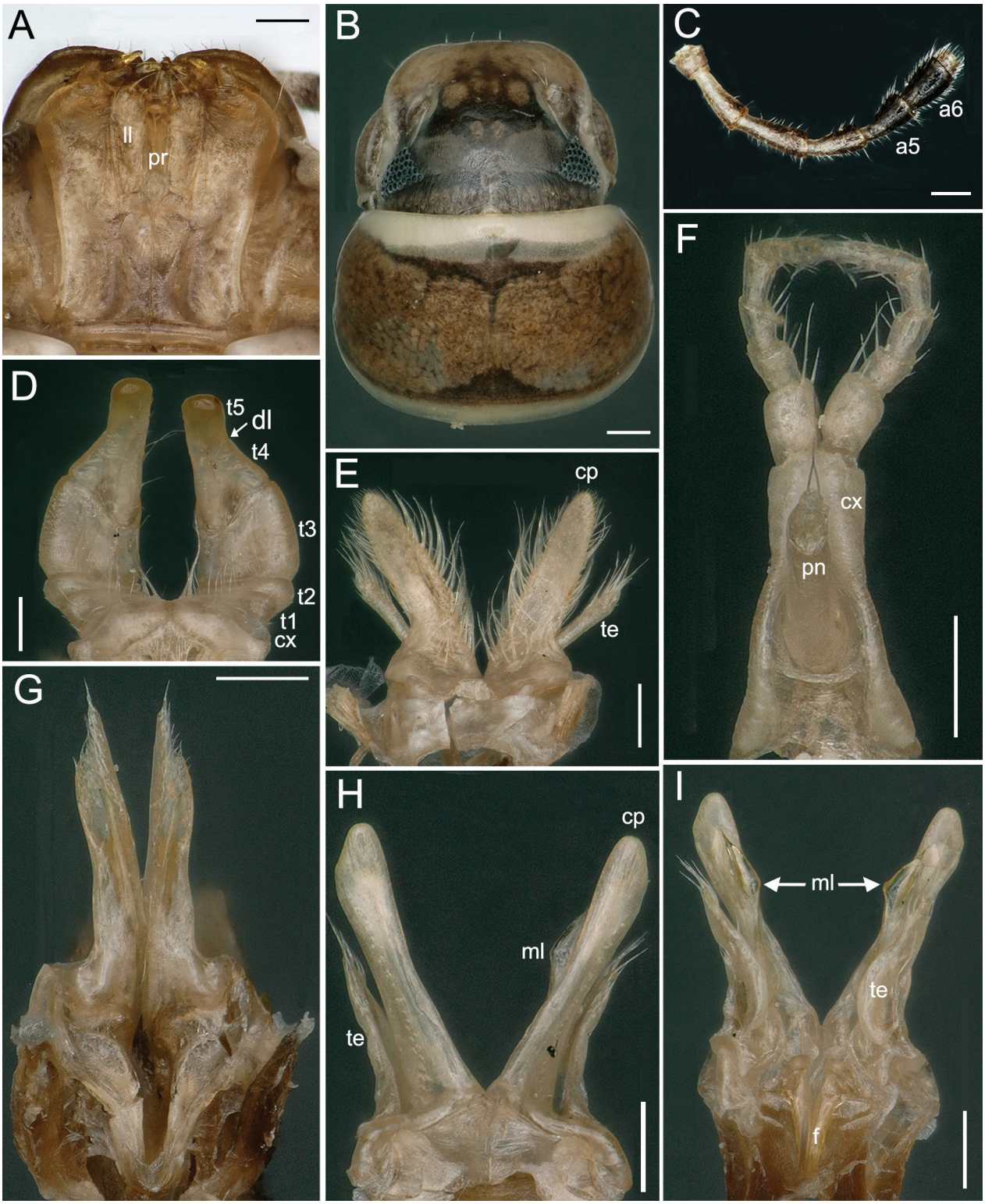

Figure 4. *Skleroprotopus yutiantianae* **sp. nov.**, holotype. **A** gnathochilarium; **B** head and collum, dorsal view; **C** left antenna, lateral view; **D** legs 1, anterior view; **E** legs 7, anterior view; **F** legs 2 with penis, posterior view; **G** posterior gonopods, anterior view; **H** anterior gonopods, anterior view; **I** anterior gonopods, posterior view. **Abbreviations:** a5, a6, antennomeres 5, 6; cp, coxal process; cx, coxa; dl, dividing line; f, flagellum; ll, lamella lingualis; ml, membranous lobe; pn, penis; pr, prementum; t1–t5, telopoditomeres 1–5; te, telopodite. **Scale bars:** 0.2 mm.

Epiproct slightly protruding caudad, with 2+2 setae along posterior margin. Paraprocts convex, medially with 2+2 setae. Hypoproct eye-shaped, with 1+1 setae.

Legs (Fig. 3F) short, about 0.7× as long as mid-body height, claw weakly curved, without modifications. Male leg-pair 1 (Fig. 4D) hypertrophied, strongly curved anteriad, 6-segmented, but dividing line (**dl**) between telopoditomeres 4 and 5 (**t4**, **t5**) incomplete. Both **t4** and **t5** combined longest, irregularly shaped, with a few scattered setae and short bristles medially. Coxa

(**cx**) and telopoditomeres 1 and 2 (**t1**, **t2**) with some long setae. Telopoditomere 3 (**t3**) broadest. Male leg-pair 2 (Fig. 4F) reduced in size and slender; penis (**pn**) unpaired, shorter than coxae (**cx**), cylindrical, distal part with two long setae. Male leg-pair 7 (Fig. 4E) strongly modified, with 2-segmented telopodites, club-shaped, densely setose apically, telopoditomere 2 rather small. Coxal process (**cp**) strongly elongated, tongue-shaped, about 2× as long as telopodite (**te**), clothed with dense long bristles.

Anterior gonopods (Fig. 4H, I) with a very long and rather slender coxal process (**cp**) bearing a long row of short villi in anterior view, posteriorly carrying with an irregularly dentate membranous lobe (**ml**), outer margin of **ml** distinctly broadened and reflexed, subtriangular, distally sharp. Flagellum (**f**) long and slender, a little barbed. Telopodite (**te**) about 2/3 as long as **cp**, with long setae apically.

Posterior gonopods (Fig. 4G) erect and thin, anterior branch slender, tapering regularly towards tip, higher than posterior branch, and both densely setose distally.

Female unknown.

Remarks. The Nanshan Park, Xining City, Qinghai Province is nicely forested in 80% of its area, dominated by hardwood tree species including *Picea crassifolia* Kom., 1923, *Juniperus przewalskii* Kom., 1924 and *Pinus tabuliformis* Carrière, 1867. The holotype of *Skleroprotopus yutiantianae* **sp. nov.** was found in forest litter.

3.3.2. *Skleroprotopus tiankeng* sp. nov.

https://zoobank.org/A91F4660-B1BD-46C3-BE71-FF0FEAB0427E

Figures 2E, 3C, 5

Material examined. Holotype male (SCAU), China, Shaanxi Province, Hanzhong City, Nanzheng District, Cave Xigoutiankeng Dong, 32°49′37.91″N 107°1′37.77″E, 850 m, 6.IX.2017, Tian Mingyi, Huang Sunbin, Wang Dianmei and Yin Haomin leg. Paratypes: 4 males, 8 females (SCAU), same data as for holotype.

Diagnosis. Differs from congeners mostly based on the following combination of characters: (1) penis much longer than coxae 2 (Fig. 5I); (2) male leg 7 with a very small coxal process, lower than the telopodite (Fig. 5E); (3) anterior gonopod (Fig. 5G, H) with a large and foot-shaped like coxal process, carrying a broadened membranous lobe, outer margin with a triangular protrusion, and a relatively thick flagellum. — In addition, this new species differs from all other species analyzed in a >10.3% uncorrected *p*-distance of the COI barcoding gene.

Etymology. The species is named after its type locality that is the Hanzhong sinkhole group, a geological wonder composed of multiple heavenly pits. “Tiankeng” in Chinese “天坑”, a noun in apposition.

Description. Length of both sexes ca 29.0–38.9 mm, width 1.9–2.2 mm, midbody height 1.8–2.1 mm, body with 49–63 podous + 1 apodous rings + telson. Natural coloration generally yellow to brownish. Antennae and legs light yellowish (Fig. 2E). Eye patches transparent, subtriangular, arranged in 4–6 irregular rows, altogether about 18–27 (males) or 15–40 (females) ommatidia per eye patch.

Head capsule smooth and hairless, eyes slightly bulged, epicranial suture well-defined. Labral margin with 2+2 supra-labral and 8+8 labral setae. Antennae long, reaching behind to anterior of ring 4 when stretched dorsally (Fig. 3C). In length, antennomeres 3>5>2>4≈6>1≈7 (Fig. 5C). Antennomeres 5, 6 and 7 each with a distal corolla of sensilla basiconica. Mandibular stipes enlarged, with two small lobes in males, well-rounded in females. Gnathochilarium with at least 3–8 setae on each lamella lingualis (**ll**) in males; prementum (**pr**) columnar in males, anteriorly swollen and tubular in shape (Fig. 5B), vs a broad conical **pr** in females (Fig. 5A).

Collum with marbled brownish spots and 8–10 lower striae laterally, but lowest 2 striae not reaching the anterior margin. Prozona with 3 irregular subtransverse striae and metazona with 13–24 longitudinal striae laterally (Fig. 3C). Suture dividing pro- and metazona rather narrow, a nearly regular comb. Ozopores starting with ring 6, lying mid-laterally on sides of metatergites.

Epiproct slightly protruding caudad, posterior margin with 6+6 setae. Paraprocts convex, with 1+1 setae. Hypoproct eye-shaped, with 1+1 setae.

Legs long and slender, about 1.4× as long as midbody height. Male leg-pair 1 (Fig. 5D) hypertrophied, 5-segmented, strongly curved anteriad. Coxa (**cx**) and telopoditomeres 1 and 2 (**t1**, **t2**) each with few long setae, others mostly short. Telopoditomere 3 (**t3**) longest, about equivalent in length to the sum of the **cx** and **t1–2**; Telopoditomere 4 (**t4**) irregularly shaped, with several long setae subapically. Male leg-pair 2 (Fig. 5I) reduced in size; penis (**pn**) pyramid-shaped, much longer than coxae (**cx**), distal part with two long setae (Fig. 5I). Male leg-pair 7 (Fig. 5E) reduced, with 3-segmented telopodites, telopoditomere 2 (**t2**) largest and setose subapically; coxal process (**cp**) small, much lower than telopodite, densely setose at mesal margin.

Anterior gonopods (Fig. 5G, H) with a large, foot-shaped like coxal process (**cp**) bearing with a long row of short villi in anterior view, posteriorly carrying with a broadened, and high membranous lobe (**ml**), slightly shorter than **cp**, middle outer margin of **ml** with a triangular protrusion. Flagellum (**f**) very long and relatively thick, distally spinulose-villose. Telopodite (**te**) about half as long as **cp**, with long setae apically, laterobasally with a minute remnant (**r**) of a second podomere.

Posterior gonopods (Fig. 5F) erect and stout, deeply branched at tip, anterior branch smooth, with a pointed tip, higher than a densely setose posterior one.

Vulva (Fig. 5J) mostly wrapped inside a membrane, characteristic in shape, strongly elongated; operculum (**op**) longer than bursa, with two parallel rows of short setae on anterior and posterior surfaces, and with at least 10 long distal setae.

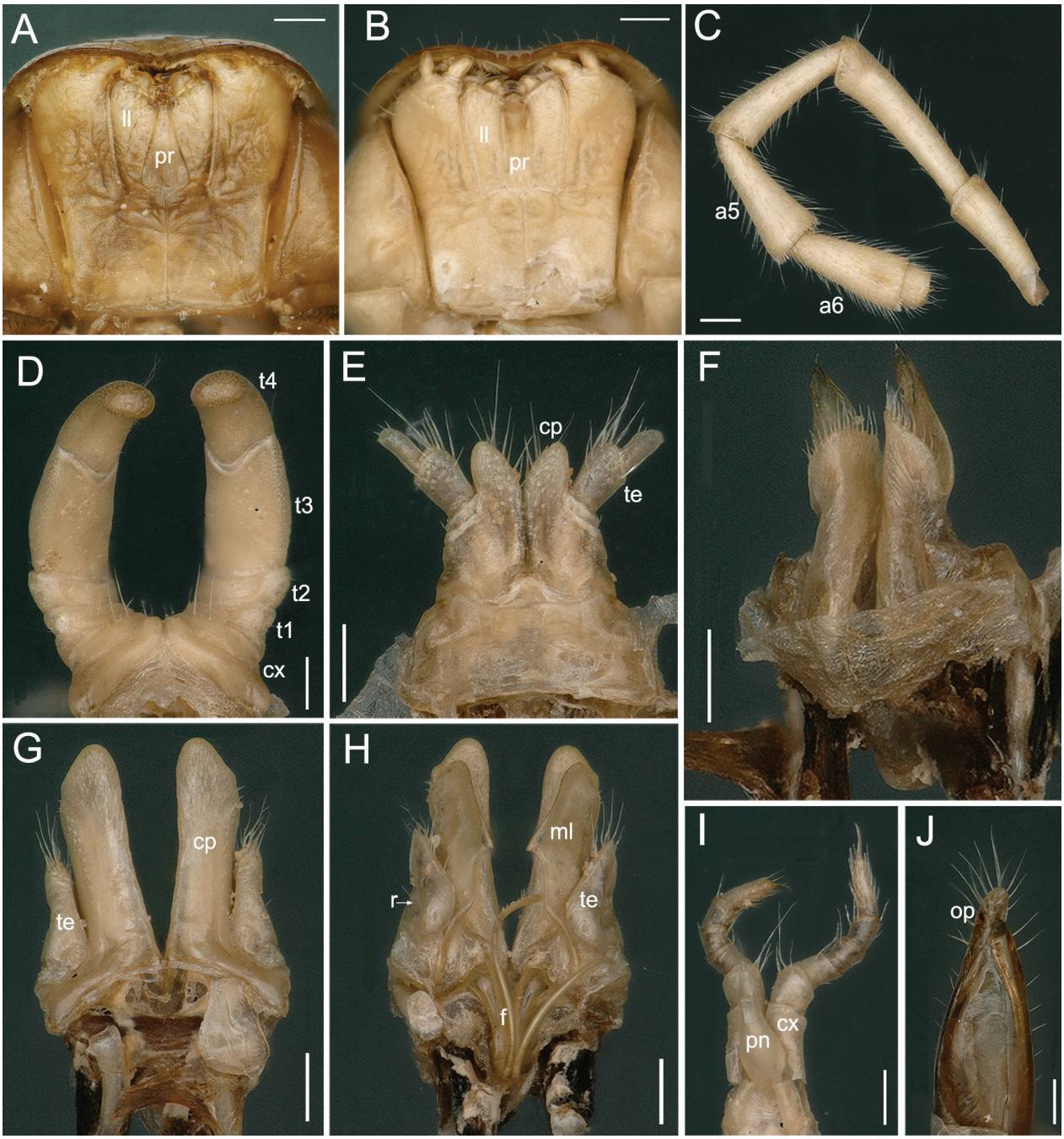

Figure 5. *Skleroprotopus tiankeng* **sp. nov.**. **A**, **J** female paratype, **B**–**I** male paratype. **A**, **B** gnathochilarium; **C** right antenna, lateral view; **D** legs 1, anterior view; **E** legs 7, anterior view; **F** posterior gonopods, posterior view; **G** anterior gonopods, anterior view; **H** anterior gonopods, posterior view; **I** legs 2 with penis, posterior view; **J** right vulva, lateral view. **Abbreviations:** a5, a6, antennomeres 5, 6; cp, coxal process; cx, coxa; f, flagellum; ll, lamella lingualis; ml, membranous lobe; op, operculum; pn, penis; pr, promentum; r, remnant; t1–t4, telopoditomeres 1–4; te, telopodite. **Scale bars:** 0.2 mm.

Remarks. The geological relic resources of Sinkhole Group at Hanzhong are mainly distributed within Xiaonanhai Town of Nanzheng District, Luojiaba Town of Xixiang County, Chanjiayan Town of Ningqiang County, and Sanyuan Town of Zhenba County, with a total area of about 5019 km^2. This new species lives in Xigoutiankeng Dong of Xiaonanhai Town, a cave that is about to be developed to the public. Based on the unpigmented body, transparent eyes, as well as long legs, *S. tiankeng* **sp. nov.** is considered a troglobite.

3.3.3. *Skleroprotopus megistus* sp. nov.

https://zoobank.org/AD0571BD-3A7A-406A-8FB7-7D65A98FE640

Figures 2B, 6

Material examined. Holotype male (SCAU), China, Shaanxi Province, Xi'an City, Wangchuan County, Cave Lingyun Dong, 34°4′21.3″N 109°23′45.01″E, 900 m, 14.IX.2017, Tian Mingyi, Huang Sunbin,

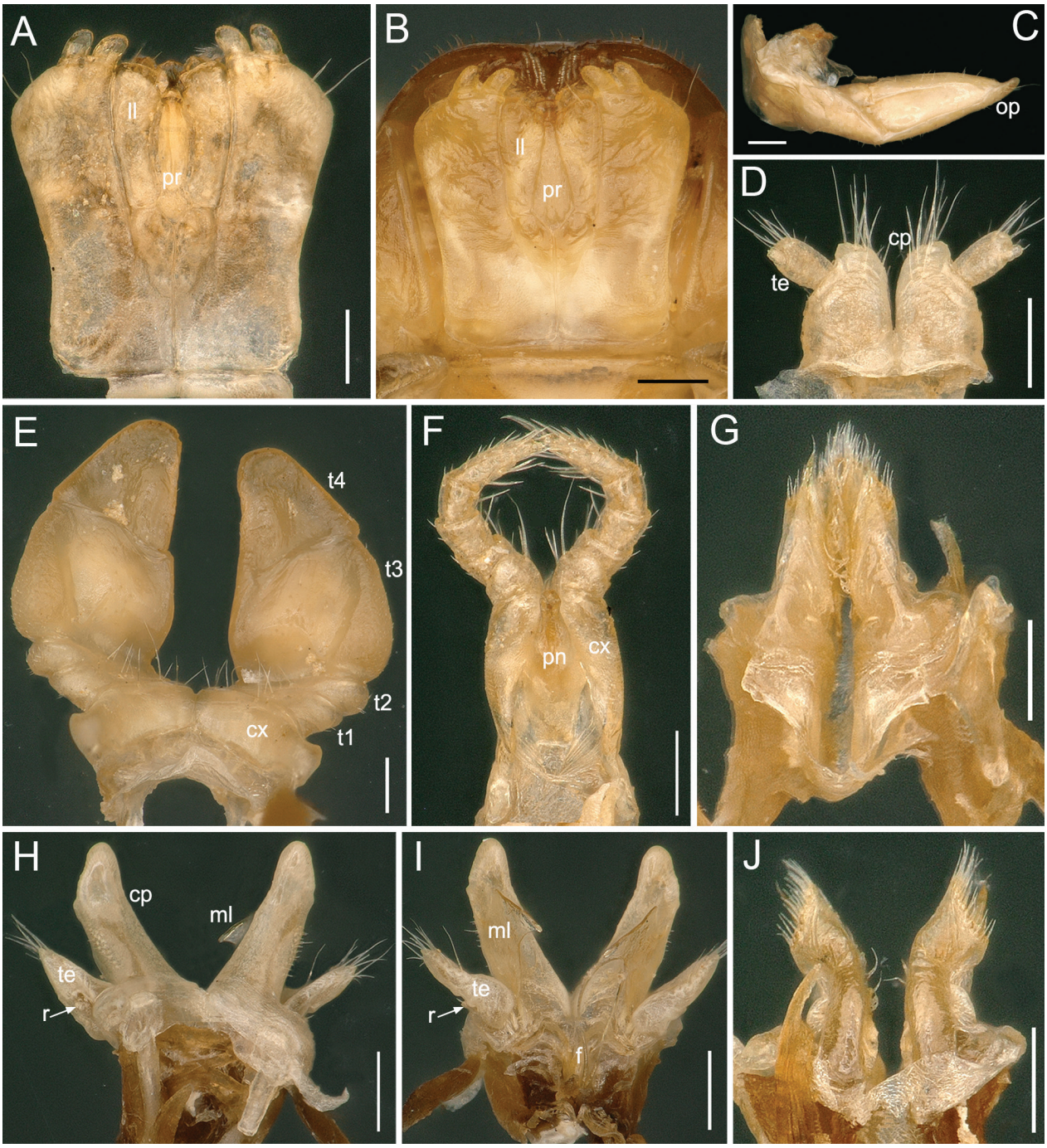

Figure 6. *Skleroprotopus megistus* **sp. nov.**. **A**, **D**–**J** male paratype; **B**, **C** female paratype. **A**, **B** gnathochilarium; **C** left vulva, lateral view; **D** legs 7, anterior view; **E** legs 1, anterior view; **F** legs 2 with penis, posterior view; **G** posterior gonopods, anterior view; **H** anterior gonopods, anterior view; **I** anterior gonopods, posterior view; **J** posterior gonopods, posterior view. **Abbreviations:** cp, coxal process; cx, coxa; f, flagella; ll, lamella lingualis; ml, membranous lobe; op, operculum; pn, penis; pr, promentum; r, remnant; t1-t4, telopoditomeres 1-4; te, telopodite. **Scale bars:** 0.2 mm.

Wang Dianmei and Yin Haomin leg. Paratypes: 6 males, 2 females (SCAU), same data as for holotype.

Diagnosis. Differs from congeners mostly based on the following combination of characters: (1) telopoditomere 3 of male leg 1 particularly broad and bulging in the middle (Fig. 6E); (2) penis subequal in height to coxae 2 (Fig. 6F); (3) coxal process of male leg 7 very small, lower than the telopodite (Fig. 6D); (4) anterior gonopod with a long coxal process carrying a highly developed, axe-shaped, membranous lobe (Fig. 6I). — In addition, this new species differs from all other species analyzed in a >10.3% uncorrected *p*-distance of the COI barcoding gene.

Etymology. Latinised Greek "*megistus*" is meaning "large". The specific epithet refers to the male leg-pair 1 being particularly large; adjective.

Description. Length of both sexes ca 31.5–40.0 mm, 1.8–2.2 mm in diameter, body with 53–65 podous + 1

apodous rings + telson. Natural coloration generally pale reddish brown (Fig. 2B), in alcohol marbled yellowish brown. Antennae and legs light yellowish. Eye patches blackish, triangular, arranged in 4–6 irregular rows, altogether about 22–52 ommatidia per eye patch.

Head capsule smooth and hairless, eyes slightly bulged, epicranial suture well-defined. Labral margin with 4+4 supra-labral and 12+12 labral setae. Antennae very long and slender, reaching behind to middle of ring 5 when stretched dorsally. In length, antennomeres 3>2>4≈5>6>1>7. Antennomeres 5, 6 and 7 each with a distal corolla of sensilla basiconica. Mandibular stipes well-rounded in males, more rounded in females. Gnathochilarium with at least 5 setae on each lamella lingualis (**ll**); prementum (**pr**) lance-shaped at base, swollen anteriorly, olive-shaped in males (Fig. 6A), vs a narrow rhomboid **pr** in females (Fig. 6B).

Collum with marbled brownish spots and 8–10 lower striae laterally, but lowest 3 striae not reaching the anterior margin. Prozona with 3–4 subtransverse striae and metazona with 13–22 longitudinal striae laterally. Suture dividing pro- and metazona very narrow, a regular comb. Ozopores starting with ring 6, lying mid-laterally on sides of metatergites (Fig. 2B).

Epiproct slightly protruding caudad, posterior margin with 3+3 setae. Paraprocts convex, medially with 1+1 setae. Hypoproct eye-shaped, with 1+1 setae.

Legs medium-sized, about as long as midbody height. Male leg-pair 1 (Fig. 6E) hypertrophied, 5-segmented, tip slightly curved anteriad. Coxa (**cx**) and telopoditomeres 1 and 2 (**t1**, **t2**) with some long setae. Telopoditomere 3 (**t3**) widest and largest, bulging in the middle. Telopoditomere 4 (**t4**) subtriangular; **t3** and **t4** devoid of long setae. Male leg-pair 2 (Fig. 6F) reduced in size; penis (**pn**) subequal in height to coxae (**cx**), distal part with three long setae. Male leg-pair 7 (Fig. 6D) reduced, with 2-segmented telopodites (**te**), **t1** large and setose subapically; coxal process (**cp**) very small, lower than telopodite (**te**), with several long setae distally.

Anterior gonopods (Fig. 6H, I) with a very long coxal process (**cp**) bearing an oval field of short villi in anterior view, posteriorly carrying with a highly developed, axe-shaped, membranous lobe (**ml**), slightly lower than **cp**, outer margin of **ml** with a large, sharp and triangular protrusion, clearly wider than **cp**. Flagellum (**f**) very long and slender, villose in distal part. Telopodite (**te**) about half as long as **cp**, with long setae apically, laterobasally with a minute remnant (**r**) of a second podomere.

Posterior gonopods (Fig. 6G, J) stout, anterior branch slender and with a small pointed tip, posterior one semi-annulate and densely setose distally.

Vulva (Fig. 6C) as usual, with two parallel rows of short setae on anterior and posterior surfaces, and two long distal setae on operculum (**op**).

Remarks. Lingyun Dong is a karst cave open to the public in the Wangchuan Scenic Area, which is about 500 meters long. Based on the unpigmented body and long antennae, *S. megistus* **sp. nov.** is considered a troglobite.

3.3.4. *Skleroprotopus longiflagellatus* sp. nov.

https://zoobank.org/AB4EB3E0-052A-43E6-A6B1-D42CE977531D

Figures 3B, 7

Material examined. Holotype male (SCAU), China, Henan Province, Nanyang City, Neixiang County, Qiliping Town, Cave Tianxin Dong, 33°20′51.85″N 111°52′56.84″E, 300 m, 30.VII.2018, Chen Mengzhen and Zhang Yan leg. Paratypes: 1 male, 8 females (SCAU), same data as for holotype.

Diagnosis. Differs from congeners mostly based on the following combination of characters: (1) penis much shorter than male coxae 2 (Fig. 7E); (2) male leg 7 strongly reduced, with a rather small coxal process and a very small telopodite (Fig. 7F); (3) anterior gonopod (Fig. 7G, H) with a very long coxal process carrying a much lower and narrow membranous lobe, outer margin with an obvious groove and (4) an extremely long and slender flagellum, higher than coxal process. — In addition, this new species differs from all other *Skleroprotopus* species analyzed in uncorrected *p*-distances ranging between 6.6% (compared to *S. change* **sp. nov.**) and 16.2% (compared to *S. longissimus* **sp. nov.**).

Etymology. The specific epithet refers to the anterior gonopod flagellum being particularly long; adjective.

Description. Length of males ca 24.0–28.5 mm, 1.7–1.8 mm in diameter, body with 47–59 podous + 1–2 apodous rings + telson. Length of females ca 30.0–37.0 mm, height 1.8–2.0 mm in diameter, body with 57–66 podous + 1 apodous rings + telson. Coloration in alcohol (Fig. 3B) uniformly dark brown, prozona dark brownish, metazona yellow. Antennae and legs brownish. Eye patches blackish, subtriangular, arranged in 5–7 irregular rows, altogether about 25–55 ommatidia per eye patchr.

Head capsule smooth and hairless, eyes slightly bulged, epicranial suture well-defined. Labral margin with about 26 setae in the first row and 4 setae in the second row. Antennae of medium length, reaching behind to anterior of ring 3 when stretched dorsally. In length, antennomeres 3>2>4>5>6>1>7. Antennomeres 5 and 6 each with a distal corolla of sensilla basiconica. Mandibular stipes well-rounded, more strongly rounded in females. Gnathochilarium with at least 4 setae on each lamella lingualis (**ll**); prementum (**pr**) lanceolate, swollen anteriorly in males (Fig. 7A), vs a drop-shaped **pr** in females (Fig. 7B).

Collum (Fig. 3B) with 5–7 lower striae laterally, but lowest 2 striae not reaching the anterior margin. Prozona with 2–5 irregular subtransverse striae and metazona with 14–18 longitudinal striae laterally. Suture dividing pro- and metazona very narrow, a regular comb. Ozopores starting with ring 6, lying mid-laterally on sides of metatergites (Fig. 3B).

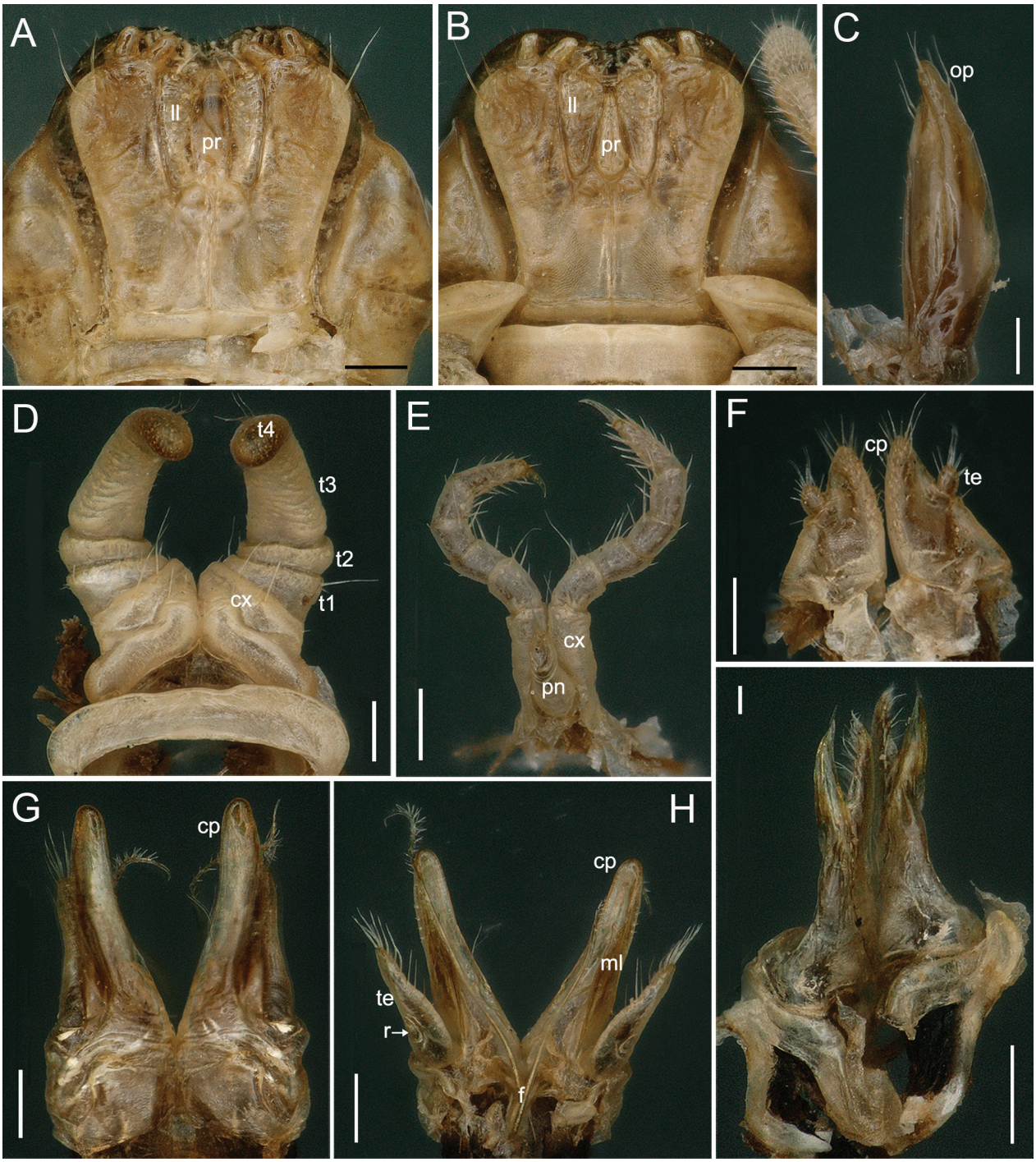

Figure 7. *Skleroprotopus longiflagellatus* **sp. nov.**. **A**, **D**–**I** male paratype; **B**, **C** female paratype. **A**, **B** gnathochilarium; **C** left vulva, lateral view; **D** legs 1, anterior view; **E** legs 2 with penis, posterior view; **F** legs 7, anterior view; **G** anterior gonopods, anterior view; **H** anterior gonopods, posterior view; **I** posterior gonopods, anterior view. **Abbreviations:** cp, coxal process; cx, coxa; f, flagella; ll, lamella lingualis; ml, membranous lobe; op, operculum; pn, penis; pr, promentum; r, remnant; t1–t4, telopoditomeres 1–4; te, telopodite. **Scale bars:** 0.2 mm.

Epiproct (Fig. 3B) slightly protruding caudad, with 5+5 setae at posterior margin. Paraprocts convex, with 3+3 setae. Hypoproct eye-shaped, with 1+1 setae.

Legs short, about 0.8× as long as midbody height. Male leg-pair 1 (Fig. 7D) hypertrophied, 5-segmented, strongly curved anteriad; coxa (**cx**) and telopoditomeres 1 and 2 (**t1**, **t2**) with some long setae. Telopoditomere 3 (**t3**) longest, about as long as all other telopoditomeres combined. Telopoditomere 4 (**t4**) irregularly shaped, midpoint slightly concave and with several long setae caudally. Male leg-pair 2 (Fig. 7E) reduced in size and slender; penis (**pn**) much shorter than coxae (**cx**), distal part with three long setae. Male leg-pair 7 (Fig. 7F) strongly reduced, each leg with 1-segmented telopodite, setose apically; coxal process (**cp**) rather small, higher than telopodite, medial margin and distally densely setose.

Anterior gonopods (Fig. 7G, H) with a very long and narrow coxal process (**cp**) bearing a long row of short

villi laterally, posteriorly carrying with a narrow, much lower membranous lobe (**ml**), outer margin of **ml** somewhat broadened, but smooth, with an obvious groove distally. Flagellum (**f**) extremely long and slender, slightly higher than **cp**, one side of distal part villose. Telopodite (**te**) about 3/5 as long as **cp**, with long setae both distally and mesally, laterobasally with a minute remnant (**r**) of a second podomere.

Posterior gonopods (Fig. 7I) erect and slightly stout, clearly branched at tip, anterior branch smooth, with a pointed tip; posterior one densely setose.

Vulva (Fig. 7C) as usual, with two parallel rows of short setae on anterior and posterior surfaces, operculum (**op**) with long setae distally.

Remarks. Tianxin Dong is also a sightseeing cave open to the public. Based on the pigmented body and legs, black eyes, as well as short legs, *S. longiflagellatus* **sp. nov.** is rather to be considered as a troglophile.

3.3.5. *Skleroprotopus change* sp. nov.

https://zoobank.org/39654E10-E972-47FA-A1EA-638D765FAD04

Figures 2A, 3H, 8

Material examined. Holotype male (SCAU), China, Hubei Province, Xianning City, Xian'an District, Chang'e Scenic Park, Cave Feixian Dong, 29°43′56.29″N 114°14′2.86″E, 160 m, 13.VII.2019, Tian Mingyi, Cheng Jingli, Chen Mengzhen and Ma Zijun leg. Paratypes: 1 male, 4 females (SCAU), same data as for holotype.

Diagnosis. Differs from congeners mostly based on the following combination of characters: (1) telopoditomere 4 of male leg 1 rounded, with a small mesal hump (Fig. 8E); (2) penis slightly longer than male coxae 2 (Fig. 8D); (3) male leg 7 with a very small coxal process and a 4-segmented telopodite (Fig. 8F); (4) anterior gonopod (Fig. 8G, H) with a very long coxal process carrying a somewhat broadened and dentated membranous lobe. — In addition, this new species differs from all other *Skleroprotopus* species analyzed in uncorrected *p*-distances ranging from between 6.6% (compared to *S. longiflagellatus* **sp. nov.**) and 15.6% (compared to *S. longissimus* **sp. nov.**).

Etymology. The specific epithet is primarily derived from its type locality, which is named after Chang'e. She is the fairy of the moon palace in the ancient Chinese mythology. "Change" in Chinese "嫦娥", a noun in apposition.

Description. Length of both sexes ca 20.5–28 mm, width 1.7–1.8 mm, midbody height 1.5–1.8 mm, body with 48–56 podous + 1–2 apodous rings + telson. Natural coloration marbled reddish- to purple brownish (Fig. 2A). Anterior 2/3 body in alcohol yellowish brown, posterior 1/3 body yellowish. Antennae and legs pale yellowish (Fig. 3H). Eye patches blackish, subtriangular, arranged in 4–6 irregular rows, altogether about 15–30 ommatidia per eye patch.

Head capsule smooth and hairless, eyes slightly bulged, epicranial suture well-defined. Labral margin with 2(3)+2(3) supra-labral and 11+11 labral setae. Antennae of medium length, reaching behind to middle of ring 2 when stretched dorsally. In length, antennomeres 3≈2>6≈5>4>1>7. Antennomeres 5 and 6 each with a distal corolla of sensilla basiconica. Mandibular stipes well-rounded in males, more strongly rounded in females. Gnathochilarium with at least 5 setae on each lamella lingualis (**ll**); prementum (**pr**) lanceolate, slightly swollen anteriorly in males (Fig. 8A), vs a narrow drop-shaped **pr** in females (Fig. 8B).

Collum with 6–8 lower striae laterally, but lowest 2 striae not reaching the anterior margin (Fig. 3H). Prozona with 4 irregular subtransverse striae and metazona with 13–17 longitudinal striae laterally. Suture dividing pro- and metazona very narrow, a regular comb. Ozopores starting with ring 6, lying mid-laterally on sides of metatergites (Fig. 3H).

Epiproct slightly protruding caudad, laterally with 2+2 setae. Paraprocts convex, smooth. Hypoproct eye-shaped, with 1+1 setae.

Legs short, about 0.6× as long as midbody height, claw weakly curved, without modifications. Male leg-pair 1 (Fig. 8E) hypertrophied, 5-segmented, strongly curved anteriad; coxa (**cx**) and telopoditomeres 1 and 2 (**t1**, **t2**) with some long setae. Telopoditomere 3 (**t3**) longest, about as long as all other telopoditomeres combined. Telopoditomere 4 (**t4**) irregularly shaped, with a small mesal hump (**h**) subapically; **t3** and **t4** with few scattered setae and short bristles on mesal face. Male leg-pair 2 (Fig. 8D) reduced in size and slender; penis (**pn**) unpaired, slightly longer than coxae (**cx**), cylindrical, distal part undulating, with five long setae. Male leg-pair 7 (Fig. 8F) strongly reduced, each leg with a 4-segmented asymmetrical telopodite (not including claw); coxal process (**cp**) small, densely setose.

Anterior gonopods (Fig. 8G, H) with a very long coxal process (**cp**) bearing two long rows of short villi in anterior view, posteriorly carrying with a membranous lobe (**ml**), outer margin of **ml** somewhat broadened, with small and irregular denticulations. Flagellum (**f**) very long and slightly thickened, distally villose. Telopodite (**te**) about half as long as **cp**, with long setae both distally and mesally, laterobasally with a minute remnant (**r**) of a second podomere.

Posterior gonopods (Fig. 8I) erect, branched at tip, anterior branch smooth, with a pointed tip, posterior one densely setose.

Vulva (Fig. 8C) mostly wrapped inside a membrane, characteristic in shape, strongly elongated; operculum (**op**) longer than bursa, with two parallel rows of short setae on anterior face and 2 long setae distally.

Remarks. This species inhabits Feixian Dong, a cave that is open to the public. Based on the pigmented body, black eyes, as well as very short legs, *S. change* **sp. nov.** is considered a troglophile.

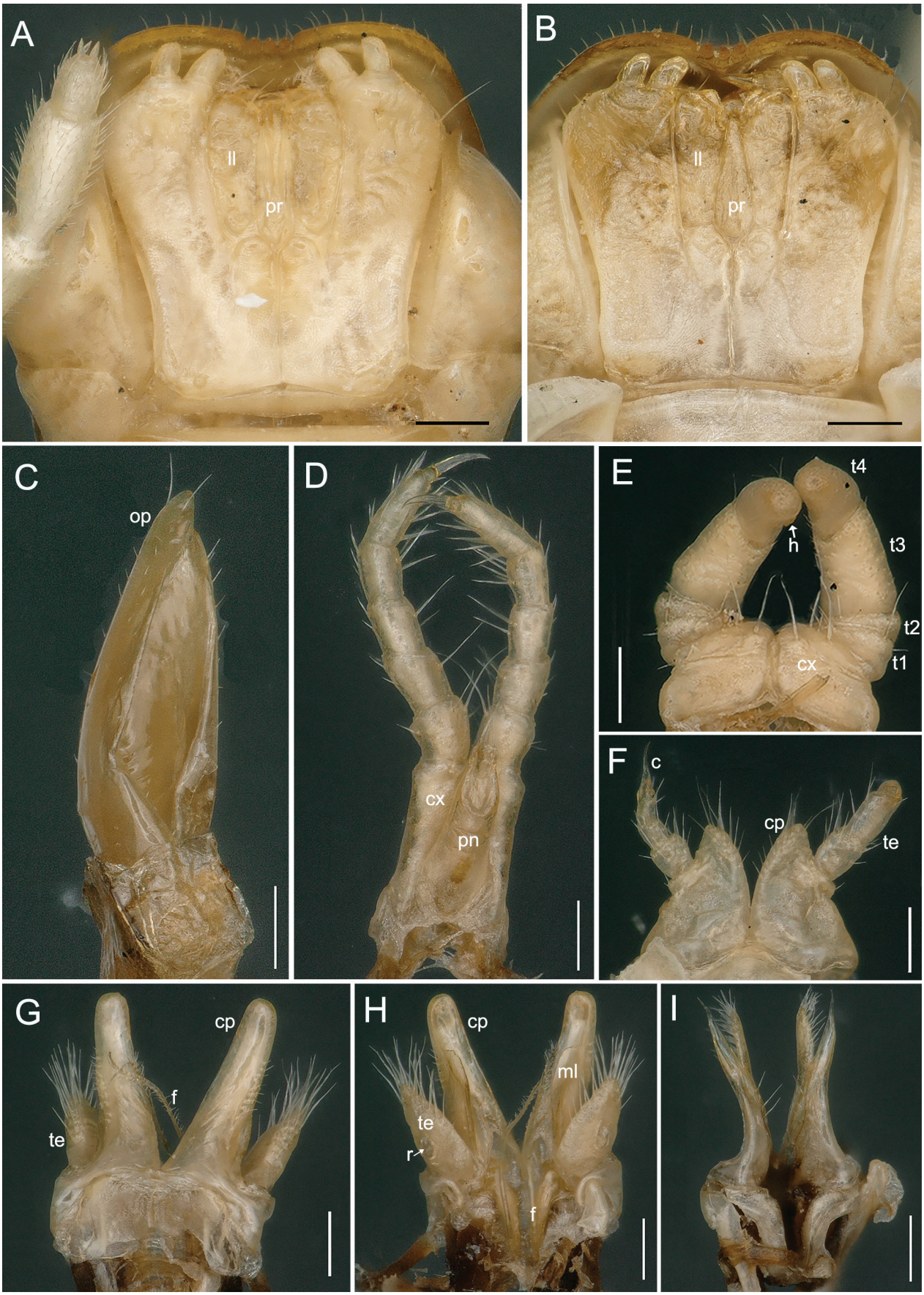

Figure 8. *Skleroprotopus change* **sp. nov.**. **A**, **D–I** male paratype; **B**, **C** female paratype. **A** gnathochilarium and part of right antenna; **B** gnathochilarium; **C** right vulva, lateral view; **D** legs 2 with penis, posterior view; **E** legs 1, anterior view; **F** legs 7, anterior view; **G** anterior gonopods, anterior view; **H** anterior gonopods, posterior view; **I** posterior gonopods, anterior view. **Abbreviations:** cp, coxal process; cx, coxa; f, flagellum; h, hump; ll, lamella lingualis; ml, membranous lobe; op, operculum; pn, penis; pr, promentum; r, remnant; t1–t4, telopoditomeres 1–4; te, telopodite. **Scale bars:** 0.2 mm.

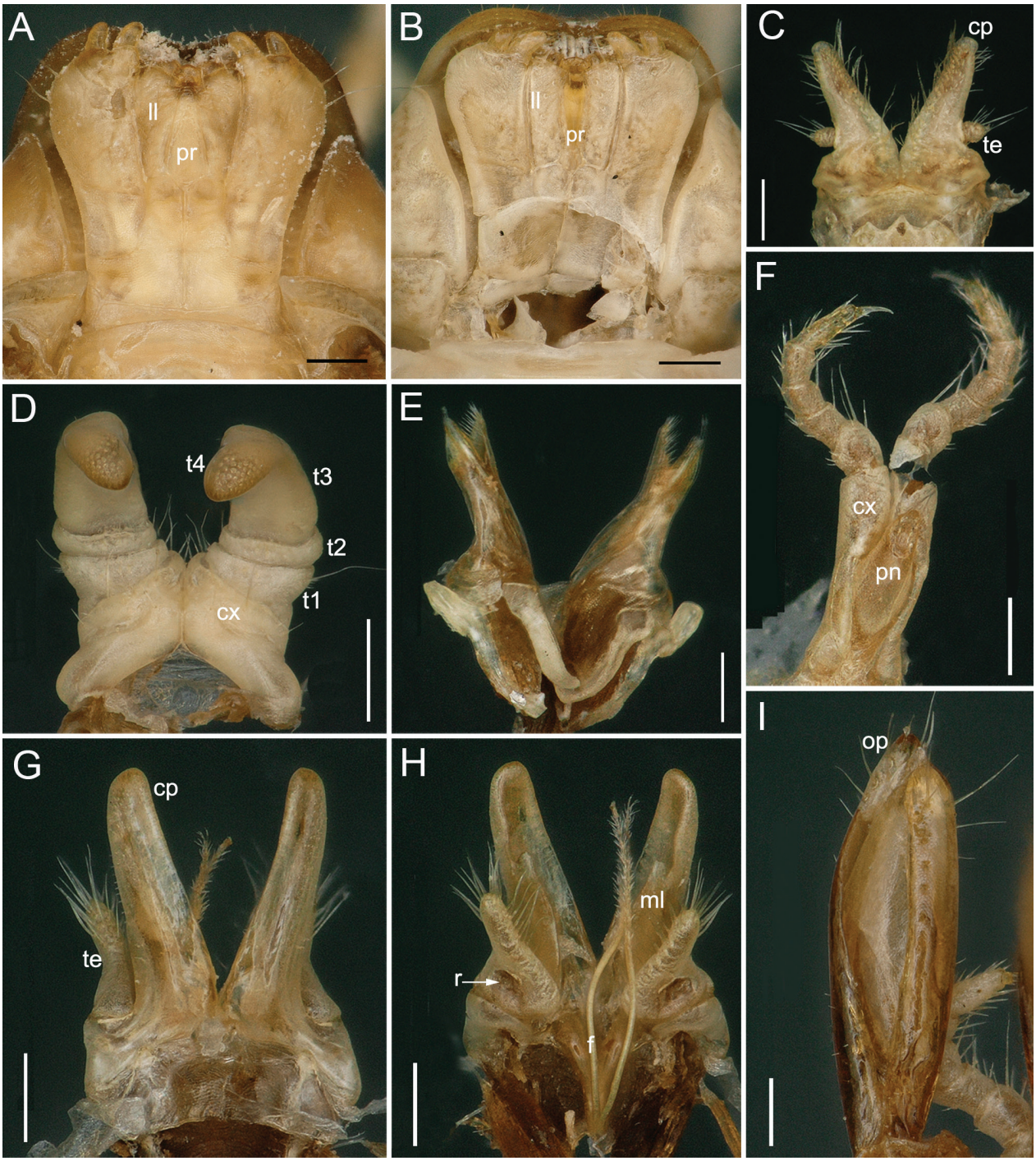

Figure 9. *Skleroprotopus penglai* **sp. nov.**. **A**, **I** female paratype; **B**–**H** male paratype. **A**, **B** gnathochilarium; **C** legs 7, anterior view; **D** legs 1, anterior view; **E** posterior gonopods, anterior view; **F** legs 2 with penis, posterior view; **G** anterior gonopods, anterior view; **H** anterior gonopods, posterior view; **I** left vulva, mesal view. **Abbreviations:** cp, coxal process; cx, coxa; f, flagellum; ll, lamella lingualis; ml, membranous lobe; op, operculum; pn, penis; pr, promentum; r, remnant; t1–t4, telopoditomeres 1–4; te, telopodite. **Scale bars:** 0.2 mm.

3.3.6. *Skleroprotopus penglai* sp. nov.

https://zoobank.org/97065E2B-1FCA-439D-A73E-72395C2E341E

Figures 3A, 9

Material examined. Holotype male (SCAU), China, Anhui Province, Chizhou City, Shitai County, Gongxi Town, Cave Penglaixian Dong, 30°13′43.57″N 117°32′7.44″E, 100 m, 17.VII.2014, Tian Mingyi, Li Wenbo and Wu Yunhe leg. Paratypes: 12 males, 5 females (SCAU), same data as for holotype.

Etymology. The name is derived from the overseas immortal mountains in Chinese mythology to emphasize the local cave harboring this species. “Penglai” in Chinese “蓬莱”, a noun in apposition.

Diagnosis. Differs from congeners mostly based on the following combination of characters: (1) penis much shorter than coxae 2 (Fig. 9F); (2) male leg 7 with a very long coxal process and a rather small telopodite (Fig. 9C); (3) anterior gonopod (Fig. 9G, H) with a very long coxal process carrying a much lower, distally grooved membranous lobe, and a very long and thick flagellum. — In addition, this new species differs from all other species analyzed in a >10.1% uncorrected *p*-distance of the COI barcoding gene.

Description. Length of both sexes ca 20.0–36.5 mm, 1.5–1.9 mm in diameter, body with 50–62 podous + 1–3 apodous rings + telson. Coloration in alcohol (Fig. 3A) uniformly brown yellowish, prozona dark brownish, metazona yellow. Antennae and legs light yellowish. Eye patches blackish, subtriangular, arranged in 5–7 irregular rows, altogether about 22–39 ommatidia per eye patch.

Head capsule smooth and hairless, eyes slightly bulged, epicranial suture well-defined. Labral margin with 2(3)+2(3) supra-labral and 7+7 labral setae. Antennae of medium length, reaching behind to middle of ring 2 when stretched dorsally. In length, antennomeres 3>2>4>5>6>7>1. Antennomeres 5 and 6 each with a distal corolla of sensilla basiconica. Mandibular stipes enlarged, with two faint lobes in males (Fig. 3A), rounded in females. Gnathochilarium with at least 6 setae on each lamella lingualis (**ll**); promentum (**pr**) lance-shaped at base, swollen anteriorly and olive-shaped in males (Fig. 9B), vs a conical **pr** in females (Fig. 9A).

Collum (Fig. 3A) with 9–11 lower striae laterally, but lowest 2 striae not reaching the anterior margin. Dorsum with 5+5 short setae at rear edge of metatergites (Fig. 3A). Prozona with 2–4 irregular subtransverse striae and metazona with 15–23 longitudinal striae laterally. Suture dividing pro- and metazona very narrow, a regular comb. Ozopores starting with ring 6, lying mid-laterally on sides of metatergites (Fig. 3A).

Epiproct slightly protruding caudad, with 4+4 setae along posterior margin. Paraprocts convex, with 3+3 setae (Fig. 3A). Hypoproct eye-shaped, with 1+1 setae.

Legs long and slender, about 1.2× as long as midbody height. Male leg-pair 1 (Fig. 9D) hypertrophied, 5-segmented, strongly curved anteriad; coxa (**cx**) and telopoditomeres 1 and 2 (**t1**, **t2**) with some long setae. Telopoditomere 3 (**t3**) longest. Telopoditomere 4 (**t4**) irregularly shaped, mid-point slightly concave. Male leg-pair 2 (Fig. 9F) reduced in size and very slender; penis (**pn**) much shorter than coxae (**cx**), distal part with three long setae. Male leg-pair 7 (Fig. 9C) strongly modified, with 2-segmented, rather small telopodites (**te**), telopoditomere 1 (**t1**) larger, with a few long setae subapically; coxal processes (**cp**) V-shaped, very long, densely setose.

Anterior gonopods (Fig. 9G, H) with a very long coxal process (**cp**) bearing a long row of short villi laterally, posteriorly carrying with a narrow, much lower, membranous lobe (**ml**), outer margin of **ml** somewhat broadened, but smooth, with an obvious groove distally. Flagellum (**f**) very long and thick, slightly shorter than **cp**, distally villose. Telopodite (**te**) about half as long as **cp**, with long setae both apically and mesally, laterobasally with a minute remnant (**r**) of a second podomere.

Posterior gonopods (Fig. 9E) erect, branched at tip, anterior branch smooth, with a pointed tip, posterior one densely setose.

Vulva (Fig. 9I) as usual, with two parallel rows of short setae on both anterior and posterior surfaces, operculum (**op**) with long setae distally.

Remarks. Penglaixian Dong is also a limestone cave open to the public, with a total length of more than 3000 meters. It consists of four floors and is an interchange structure. Based on the unpigmented body and long legs, *S. penglai* **sp. nov.** is considered a troglobite.

3.3.7. *Skleroprotopus longissimus* sp. nov.

https://zoobank.org/CEFDE092-2A67-4675-96CA-EAE15ECA79CC

Figures 2C, 10

Material examined. Holotype male (SCAU), China, Hunan Province, Chenzhou City, Guidong County, Sidu Town, Cave Bidongfeiyan Dong, 26°0′13.32″N 113°46′28.25″E, 800 m, 19.X.2013, Tian Mingyi, Liu Weixin and Yin Haomin leg. Paratypes: 1 male, 5 females, 4 juveniles (SCAU), same data as for holotype; 7 males, 13 females, 1 juvenile, same cave, 4.IV.2021, Tian Mingyi and Cheng Jingli leg. Other material examined: 4 males, 5 females, 2 juveniles (SCAU), same county, Sidu Town, Cave Sidu Dong, 25°57′46.55″N 113°47′07.33″E, 900 m, VII.2011, Tian Mingyi, Gao Qi and Sun Feifei leg.

Diagnosis. Differs from congeners mostly based on the following combination of characters: (1) penis much shorter than coxae 2 (Fig. 10E); (2) male leg-pair 7 with a rather long and slender coxal process (Fig. 10F); (3) anterior gonopod (Fig. 10G, H) with a very long coxal process carrying an irregularly dentate and membranous lobe, and a very long and slender flagellum. — In addition, this new species differs from all other species analyzed in a >12.4% uncorrected *p*-distance of the COI barcoding gene.

Etymology. Latin "*longissimus*" is meaning "the longest". The specific epithet refers to the coxal process of male leg-pair 7 being particularly long and relatively slender; ajective.

Description. Length of both sexes ca 25.0–40.0 mm, 1.6–1.9 mm in diameter, body with 47–54 podous + 1 apodous rings + telson. Natural coloration (Fig. 2C) red brownish, in alcohol uniformly brown yellowish, prozona dark brownish, metazona yellowish. Antennae and legs light yellowish. Eye patches blackish, subtriangular, arranged in 4–7 irregular rows, altogether about 20–37 ommatidia per eye patch.

Head capsule smooth and hairless, eyes slightly bulged, epicranial suture well-defined. Labral margin with 2(3)+2(3) supra-labral and 9+9 labral setae. An-

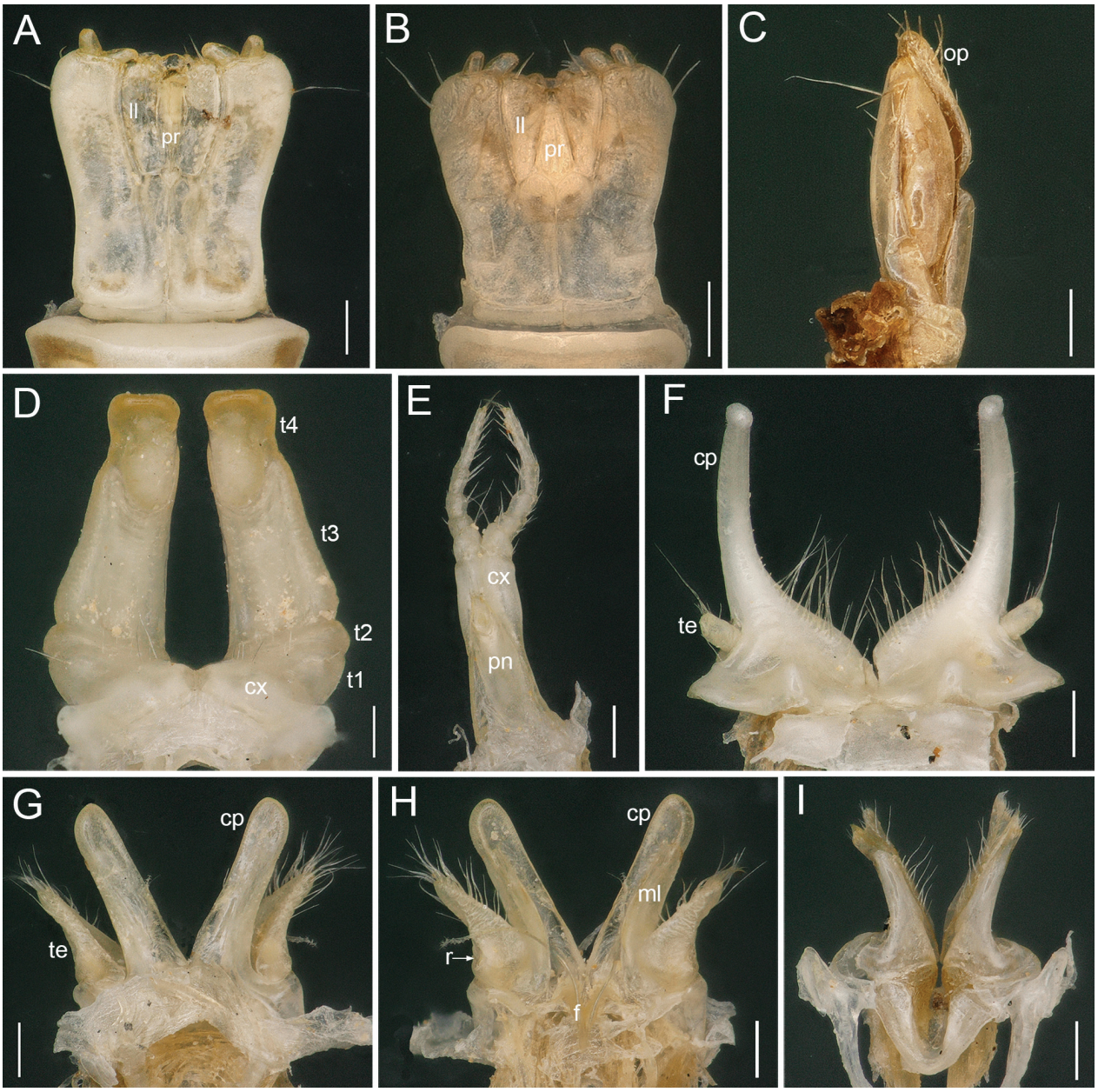

Figure 10. *Skleroprotopus longissimus* **sp. nov.**. paratypes from Cave Bidongfeiyan Dong. **A**, **D**–**I** male paratype; **B**, **C** female paratype. **A**, **B** gnathochilarium; **C** right vulva, mesal view; **D** legs 1, anterior view; **E** legs 2 with penis, posterior view; **F** legs 7, anterior view; **G** anterior gonopods, anterior view; **H** anterior gonopods, posterior view; **I** posterior gonopods, anterior view. **Abbreviations:** cp, coxal process; cx, coxa; f, flagellum; ll, lamella lingualis; ml, membranous lobe; op, operculum; pn, penis; pr, promentum; r, remnant; t1–t4, telopoditomeres 1–4; te, telopodite. **Scale bars:** 0.2 mm.

tennae of medium length, reaching behind to anterior of ring 3 when stretched dorsally. In length, antennomeres 3>2>4≈5>6>1>7. Antennomeres 5 and 6 each with a distal corolla of sensilla basiconica. Mandibular stipes well-rounded, with two small lobes in males, more rounded in females. Gnathochilarium with at least 4 setae on each lamella lingualis (**ll**); promentum (**pr**) relatively narrow, lance-shaped at base, swollen anteriorly and cup-shaped in males (Fig. 10A), vs a slightly broadened and oblong rhomboid **pr** in females (Fig. 10B).

Collum with 5–7 lower striae laterally, but lowest 2 striae not reaching the anterior margin. Prozona with 4–6 irregular subtransverse striae and metazona with 11–25 longitudinal striae laterally. Suture dividing pro- and metazona very narrow, a regular comb. Ozopores starting with ring 6, lying mid-laterally on sides of metatergites.

Epiproct slightly protruding caudad, with 4+4 setae at posterior margin. Paraprocts convex, with 2+2 setae. Hypoproct eye-shaped, with 1+1 setae.

Legs long and slender, about 1.1× as long as mid-body height. Male leg-pair 1 (Fig. 10D) hypertrophied, 5-segmented, strongly curved anteriad; coxa (**cx**) and telopoditomeres 1 and 2 (**t1**, **t2**) with some long setae. Telopoditomere 3 (**t3**) longest, about as long as all other telopoditomeres combined; Telopoditomere 4 (**t4**) irregularly shaped, with two vague emarginations, one lateral, the other dorsal. Male leg-pair 2 (Fig. 10E) reduced in size and very slender; penis (**pn**) shorter than coxae (**cx**),

distal part with three long setae. Male leg-pair 7 (Fig. 10F) strongly modified, coxal process (**cp**) extremely long and slender, crowned with a small hook facing anteriorly, strongly bent frontally, mostly subparallel-sided, considerably more slender, and free from setae along distal 2/3; telopodite (**te**) 1-segmented, rather small, carrying a long apical seta.

Anterior gonopods (Fig. 10G, H) with a medium length coxal process (**cp**), posteriorly carrying with an irregularly dentate membranous lobe (**ml**), outer margin of **ml** somewhat broadened and reflexed in proximal half, margin of reflexed part irregular. Flagellum (**f**) very long and slender, distally serrate and branched. Telopodite (**te**) about 3/4 as long as **cp**, with long setae both apically and mesally, laterobasally with a minute remnant (**r**) of a second podomere.

Posterior gonopods (Fig. 10I) erect, branched at tip, anterior branch smooth, with a pointed tip, posterior one densely setose.

Vulva (Fig. 10C) as usual, with two parallel rows of short setae on both anterior and posterior surfaces, operculum (**op**) with several long setae distally.

Remarks. Sidu Karst is located in the Bamianshan National Nature Reserve, being the largest cave group found so far in southern Hunan. As the antennae and legs of this species are apparently slender and unpigmented, albeit the body retains some pigment, *S. longissimus* **sp. nov.** is considered a troglobite.

3.3.8. *Skleroprotopus genjudi* sp. nov.

https://zoobank.org/84BD5B7A-81AB-472D-8FF9-82A756B27920

Figures 2D, 11

Material examined. Holotype male (SCAU), China, Jiangxi Province, Ganzhou City, Chongyi County, Niedu Town, Cave Luohanyan, 25°27′9.03″N 114°05′1.28″E, 400 m, 9.XI.2014, fifteen graduate students from the class of 2013 leg. Paratypes: 28 males, 12 females (SCAU), same data as for holotype; 6 males, 6 females (SCAU), same cave, 12.I.2011, Tian Mingyi, Liu Weixin, Zheng Yuan and Sun Feifei leg. Other material examined: 4 males, 5 females (SCAU), same town, Cave Miao Dong, 25°28′1.62″N 114°05′6.77″E, 350 m, 13.I.2011, Tian Mingyi, Liu Weixin, Zheng Yuan and Sun Feifei leg.; 3 males (SCAU), same town, Cave Lianhua Dong, 25°28′10″N, 114°05′37″E, 400 m, 16.IV.2017, fifteen graduate students from the class of 2016 leg.

Diagnosis. Differs from congeners mostly based on the following combination of characters: (1) penis much shorter than coxae 2 (Fig. 11E); (2) male leg 7 with an extremely long coxal process, strongly bent anteriad, telopodite rather small, 2 or 3-segmented (Fig. 11F); (3) anterior gonopod (Fig. 11G, H) with a coxal process of medium length and carrying a much lower, irregularly dentate, membranous lobe, and a very long and slender flagellum, distally branched. — In addition, this new species differs from all other species analyzed in a >8.2% uncorrected *p*-distance of the COI barcoding gene.

Etymology. The species name is primarily derived from its collection site, which is often used as a place for our graduate students to conduct internships on cave biodiversity. “Genjudi” here refers to the main operational base, in Chinese is “根据地”; a noun in apposition.

Description. Length of both sexes ca 30.0–42.0 mm, 1.7–2.1 mm in diameter, body with 51–63 podous + 1–2 apodous rings + telson. Natural coloration (Fig. 2D) uniformly grayish yellow. Antennae and legs light yellow. Eye patches grey to blackish, subtriangular, arranged in 4–7 irregular rows, altogether about 30–40 ommatidia per eye patch.

Head capsule smooth and hairless, eyes slightly bulged, epicranial suture well-defined. Labral margin with 1(2)+1(2) supra-labral and 11+11 labral setae. Antennae long and slender, reaching behind to middle of ring 4 when stretched dorsally. In length, antennomeres 3>2>4>5>6>1>7. Antennomeres 5 and 6 each with distal corolla of sensilla basiconica. Antennomere 7 with 4 sensory cones. Mandibular stipes enlarged, with two small lobes in males, rounded in females. Gnathochilarium with at least 7 setae on each lamella lingualis (**ll**); prementum (**pr**) lance-shaped at base, swollen anteriorly, short and rod-like in males (Fig. 11A), vs a drop-shaped **pr** in females (Fig. 11B).

Collum with 4–6 lower striae laterally, but lowest 2 striae not reaching the anterior margin. Prozona with 2–6 irregular subtransverse striae and metazona with 16–24 longitudinal striae laterally. Suture dividing pro- and metazona very narrow, a regular comb. Ozopores starting with ring 6, lying mid-laterally on sides of metatergites.

Epiproct slightly protruding caudad, posterior margin with 3+3 setae. Paraprocts convex, with 1+1 setae. Hypoproct eye-shaped, with 1+1 setae.

Legs long and slender, about 1.2× as long as mid-body height. Male leg-pair 1 (Fig. 11D) hypertrophied, 5-segmented, strongly curved anteriad; coxa (**cx**) and telopoditomeres 1 and 2 (**t1**, **t2**) with several long setae. Telopoditomere 3 (**t3**) longest, about as long as all other telopoditomeres combined. Telopoditomere 4 (**t4**) irregularly shaped, with two vague emarginations, one lateral, the other dorsal. Male leg-pair 2 (Fig. 11E) reduced in size and slender; penis (**pn**) shorter than coxae (**cx**), distal part with five long setae. Male leg-pair 7 (Fig. 11F) strongly modified, coxal process (**cp**) extremely long, flattened dorsoventrally, only slightly attenuated distad, strongly bent anteriad, densely setose nearly throughout at both mesal and lateral margins; telopodite (**te**) remains poorly visible laterally near base of **cp**, vestigial, consisting of 2 or 3 very small telopoditomeres.

Anterior gonopods (Fig. 11G, H) with a coxal process (**cp**) of medium length, laterally bearing a long row of short villi, posteriorly carrying with a lower membranous lobe (**ml**), outer margin of **ml** irregularly dentate, somewhat broadened and reflexed in proximal half. Flagellum (**f**) very long and slender, distally serrate and branched. Telopodite (**te**) about 2/3 as long as **cp**, with long setae both apically and mesally, laterobasally with a minute remnant (**r**) of a second podomere.

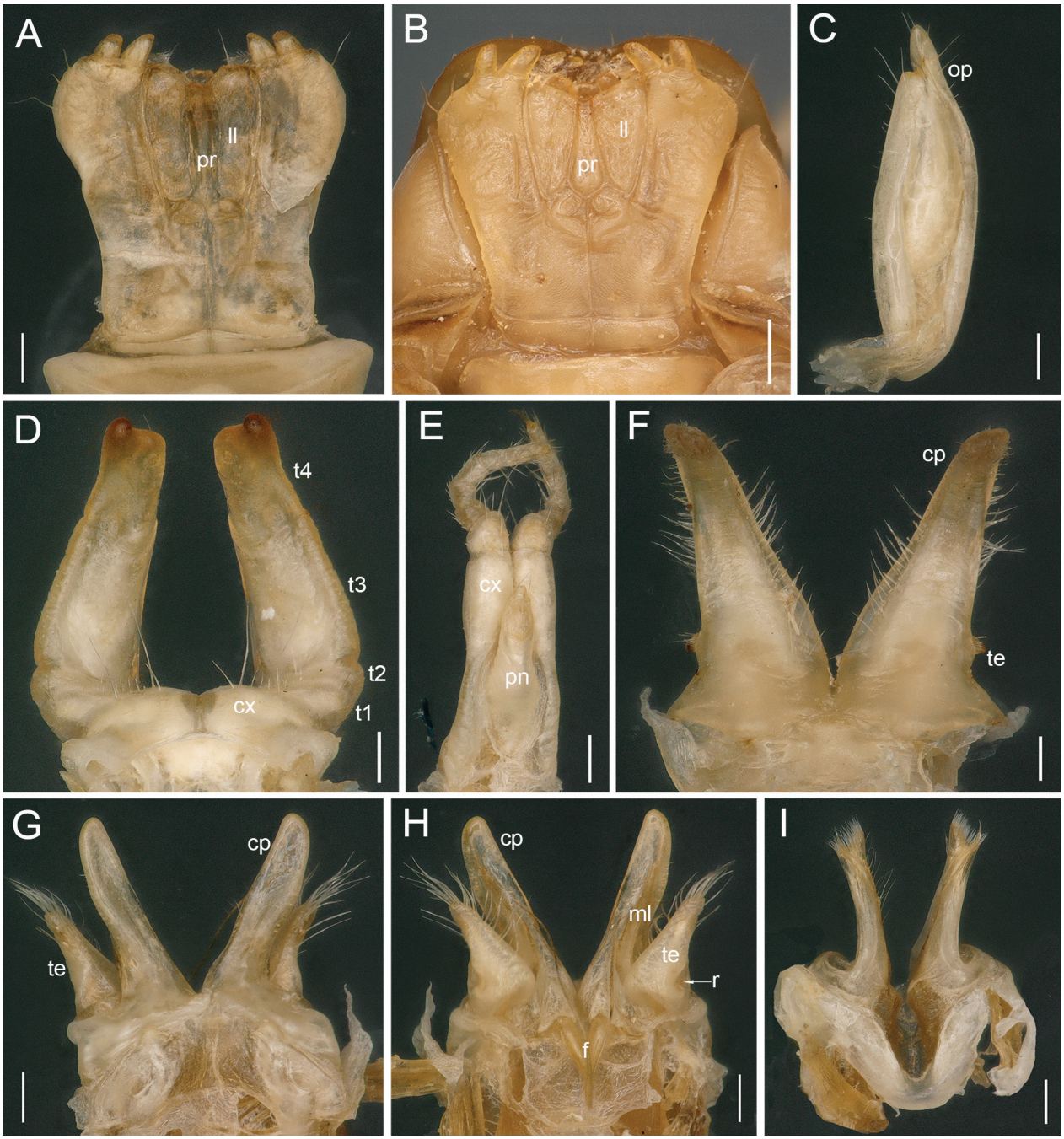

Figure 11. *Skleroprotopus genjudi* **sp. nov.**. paratypes from Cave Luohanyan. **A**, **D**–**I** male paratype; **B**, **C** female paratype. **A**, **B** gnathochilarium; **C** right vulva, mesal view; **D** legs 1, anterior view; **E** legs 2 with penis, posterior view; **F** legs 7, anterior view; **G** anterior gonopods, anterior view; **H** anterior gonopods, posterior view; **I** posterior gonopods, anterior view. **Abbreviations:** cp, coxal process; cx, coxa; f, flagellum; ll, lamella lingualis; ml, membranous lobe; op, operculum; pn, penis; pr, promentum; r, remnant; t1–t4, telopoditomeres 1–4; te, telopodite. **Scale bars:** 0.2 mm.

Posterior gonopods (Fig. 11I) erect, with bristles medially, distally branched, anterior branch smooth and slender, with a pointed tip, posterior one densely setose.

Vulva (Fig. 11C) as usual, with two parallel rows of short setae on both anterior and posterior surfaces, operculum (**op**) with several long setae distally.

Remarks. This new species was found in several caves at Niedu Town, Chouyi City, Jiangxi. Based on the unpigmented body, as well as long legs and antennae, *S. genjudi* **sp. nov.** is considered a troglobite.

3.3.9. *Skleroprotopus ampullaceus* sp. nov.

https://zoobank.org/F92A792E-A92F-4E6A-AD43-F6D72E84780F

Figures 3D, 12

Material examined. Holotype male (SCAU), China, Jiangxi Province, Shangrao City, Wuyuan County, Cave Penghua Dong, 19.VII.2014, Tian Mingyi, Wu Yunhe and Li Wenbo leg. Paratypes: 34 males, 7 females (SCAU), same data as for holotype.

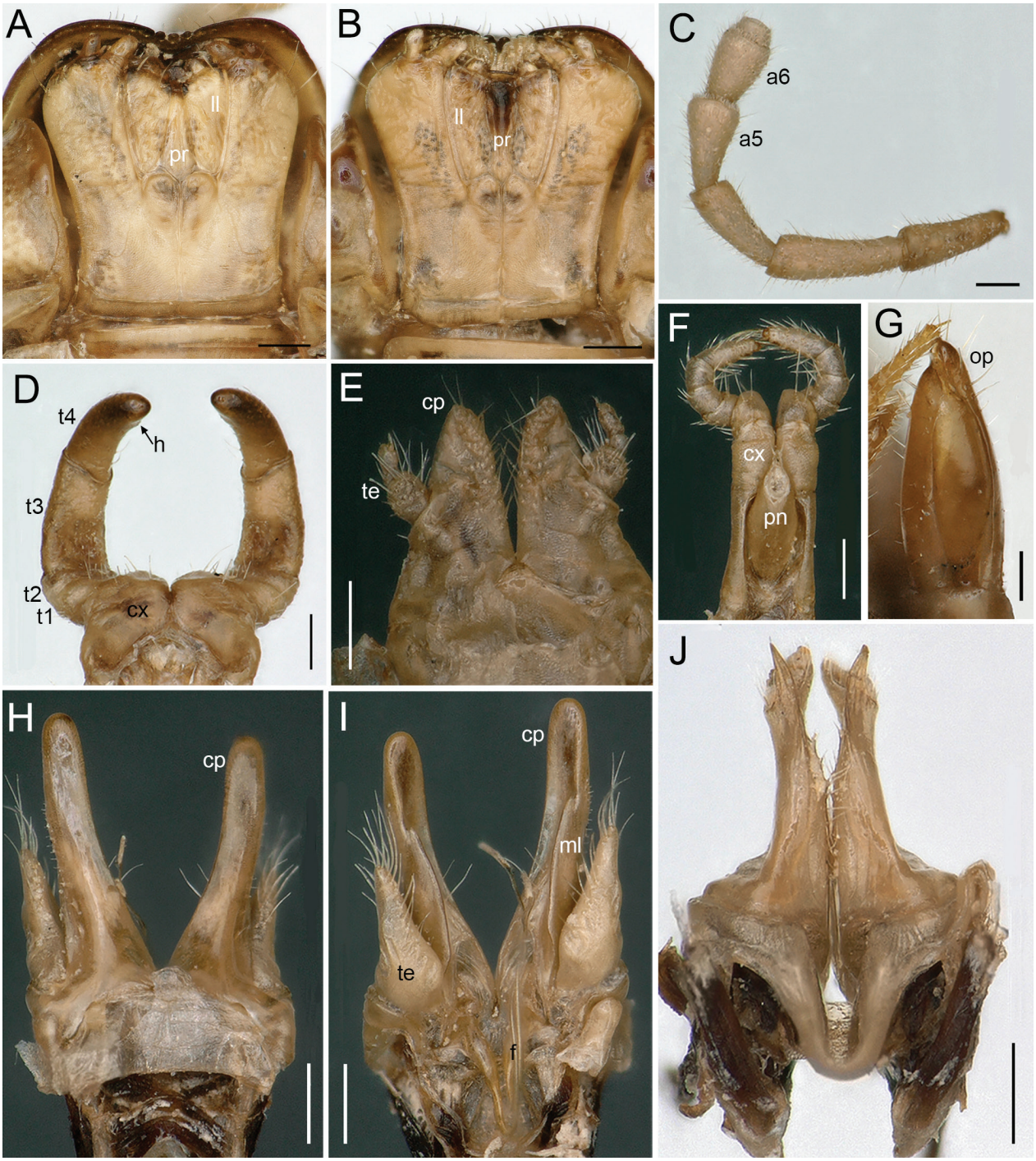

Figure 12. *Skleroprotopus ampullaceus* **sp. nov.**. **A**, **G** female paratype; **B**–**F**, **H**–**J** male paratype. **A**, **B** gnathochilarium; **C** right antenna, lateral view; **D** legs 1, anterior view; **E** legs 7, anterior view; **F** legs 2 with penis, posterior view; **G** right vulva, mesal view; **H** anterior gonopods, anterior view; **I** anterior gonopods, posterior view; **J** posterior gonopods, anterior view. **Abbreviations:** a5, a6, antennomeres 5, 6; cp, coxal process; cx, coxa; f, flagella; h, hump; ll, lamella lingualis; ml, membranous lobe; op, operculum; pn, penis; pr, promentum; r, remnant; t1–t4, telopoditomeres 1–4; te, telopodite. **Scale bars:** 0.2 mm.

Diagnosis. Differs from congeners mostly based on the following combination of characters: (1) male leg 1 relatively slender, telopoditomere 4 linguiform, with a small mesal hump (Fig. 12D); (2) penis much shorter than coxae 2 (Fig. 12F); (3) male leg 7 with a coxal process of medium size, densely setose at mesal margin, height subequal to telopodite, which is made up of 2 or 3 segements and a claw (Fig. 12E); (4) anterior gonopod (Fig. 12H, I) with a rather long coxal process carrying a narrow, lower, membranous lobe, distally with a vague indentation. — In addition, this new species differs from all other species analyzed in a >9.1% uncorrected *p*-distance of the COI barcoding gene.

Etymology. Latin "*ampullaceus*" is meaning bottle-shaped. The specific epithet refers to the the promentum of the gnathochilarium being bottle-shaped in males; adjective.

Description. Length of both sexes ca 30.0–37.0 mm, 1.8–2.0 mm in diameter, body with 48–58 podous + 1–2 apodous rings + telson. Coloration in alcohol (Fig. 3D) uniformly yellow to dark brownish. Antennae and legs yellow brownish. Eye patches blackish, subtriangular, arranged in 4–6 irregular rows, altogether about 20–38 ommatidia per eye patch.

Head capsule smooth and hairless, eyes slightly bulged, epicranial suture well-defined. Labral margin with 2(3)+2(3) supra-labral and 9+9 labral setae. Antennae of medium length, reaching behind to middle of ring 2 when stretched dorsally. In length, antennomeres 3>4>2>5>6>1>7 (Fig. 12C). Antennomeres 5 and 6 each with a distal corolla of sensilla basiconica. Mandibular stipes well-rounded, with two small lobes in male, rounded in female. Gnathochilarium with at least 5 setae on each lamella lingualis (**ll**); prementum (**pr)** lance-shaped at base, swollen anteriorly, bottle-shaped in males (Fig. 12B), vs a narrow, oblong, rhomboid **pr** in females (Fig. 12A).

Collum with 6–14 lower striae laterally, but lowest 4 striae not reaching the anterior margin. Prozona with 2–4 irregular subtransverse striae and metazona with 13–19 longitudinal striae laterally (Fig. 3D). Suture dividing pro- and metazona very narrow, a regular comb. Ozopores starting with ring 6, lying mid-laterally on sides of metatergites.

Epiproct slightly protruding caudad, with 4+4 setae at posterior margin. Paraprocts convex, with 1+1 setae. Hypoproct eye-shaped, with 1+1 setae.

Legs short, but slender, about 0.9× as long as mid-body height. Male leg-pair 1 (Fig. 12D) hypertrophied, relatively slender, 5-segmented, strongly curved anteriad; coxa (**cx**) and telopoditomeres 1 and 2 (**t1**, **t2**) with some long setae. Telopoditomere 3 (**t3**) longest, 1.5× as long as telopoditomere 4 (**t4**), **t4** linguiform, with a small mesal hump (**h**) subapically; **t3** and **t4** with long setae medially. Male leg-pair 2 (Fig. 12F) reduced in size; penis (**pn**) fat, much shorter than coxae (**cx**), distal part with two long setae. Male leg-pair 7 (Fig. 12E) reduced, each leg with a 2 or 3-segmented asymmetrical telopodite (**te**) and a claw, telopoditomere 1 (**t1**) largest and setose subapically; coxal process (**cp**) medium-sized, about as high as **te**, densely setose at mesal margin.

Anterior gonopods (Fig. 12H, I) with a very long and relatively narrow coxal process (**cp**) bearing a long row of short villi laterally, posteriorly with a narrow, lower, membranous lobe (**ml**), outer margin of **ml** smooth, with a vague indentation distally. Flagellum (**f**) very long and slender, distally villose and branched. Telopodite (**te**) about half as long as **cp**, with long setae both apically and mesally, laterobasally with a minute remnant (**r**) of a second podomere.

Posterior gonopods (Fig. 12J) erect, with bristles medially, distally branched, anterior branch smooth, with a pointed tip, posterior one densely setose.

Vulva (Fig. 12G) as usual, with two parallel rows of short setae on both anterior and posterior surfaces, operculum (**op**) with several long setae distally.

Remarks. Based on the pigmented body, black eyes, as well as moderately long legs and antennae, *S. ampullaceus* **sp. nov.** is considered a troglophile.

3.3.10. *Skleroprotopus incisodentatus* sp. nov.

https://zoobank.org/F19FF3FB-0081-4749-AA16-A7A46D-77AC87

Figures 2G, 13

Material examined. Holotype male (SCAU), Jiangxi Province, Shangrao City, Guangfeng County, Cave Lingjiu Dong, 28°27′54.12″N 118°20′39.79″, 200 m, 29.IX.2014, Huang Sunbin and Wang Xinhui leg. Paratypes: 2 males, 2 females (SCAU), same data as for holotype; 3 males, 7 females (SCAU), same county, Cave Tiangui Yan, 28°27′31.44″N 118°16′57.70″E, 200 m, 28.IX.2014; 1 male, 7 females (SCAU), Zhejiang Province, Jiangshan City, Dachen County, Cave Wulong Dong, 28°48′35.83″N 118°34′59.37″E, 300 m, 28.IX.2014, all Huang Sunbin and Wang Xinhui leg.

Diagnosis. Differs from congeners mostly based on the following combination of characters: (1) telopoditomere 4 of male leg 1 with a small mesal hump (Fig. 13D); (2) penis slightly higher than coxae 2 (Fig. 13C); (3) male leg 7 with a very small coxal process, much lower than telopodite, which is made up of 4 segments and a claw (Fig. 13F); (4) anterior gonopod (Fig. 13E, I) with a very long coxal process carrying a narrow, lower, membranous lobe, distally with a vague indentation. — In addition, this new species differs from all other species analyzed in a >8.0% uncorrected *p*-distance of the COI barcoding gene.

Etymology. The specific epithet refers to the distally vague indentation of a membranous lobe of anterior gonopod; adjective.

Description. Length of both sexes ca 26.0–44.0 mm, 1.7–2.0 mm in diameter, body with 48–68 podous + 1–2 apodous rings + telson. Natural coloration (Fig. 2G) red brownish to purple brownish; generally yellow brownish in alcohol, prozona dark brownish. Antennae and legs yellow. Eye patches blackish, subtriangular, arranged in 6–8 irregular rows, altogether about 24–48 ommatidia per eye patch.

Head capsule smooth and hairless, eyes slightly bulged, epicranial suture well-defined. Labral margin with 2+2 supra-labral and 8+8 labral setae (Fig. 13B). Antennae long and slender, reaching behind to middle of ring 4 when stretched dorsally. In length, antennomeres 3>2>4≈5>4>6>7>1. Antennomeres 5 and 6 each with a distal corolla of sensilla basiconica. (Fig. 13B). Mandibular stipes well-rounded, with two small lobes in males, regularly rounded in females. Gnathochilarium with at least 5 setae on each lamella lingualis (**ll**); prementum (**pr**) short and lanceolate, anteriorly swollen in males (Fig. 13B), vs a narrow rhombic **pr** in females (Fig. 13A).

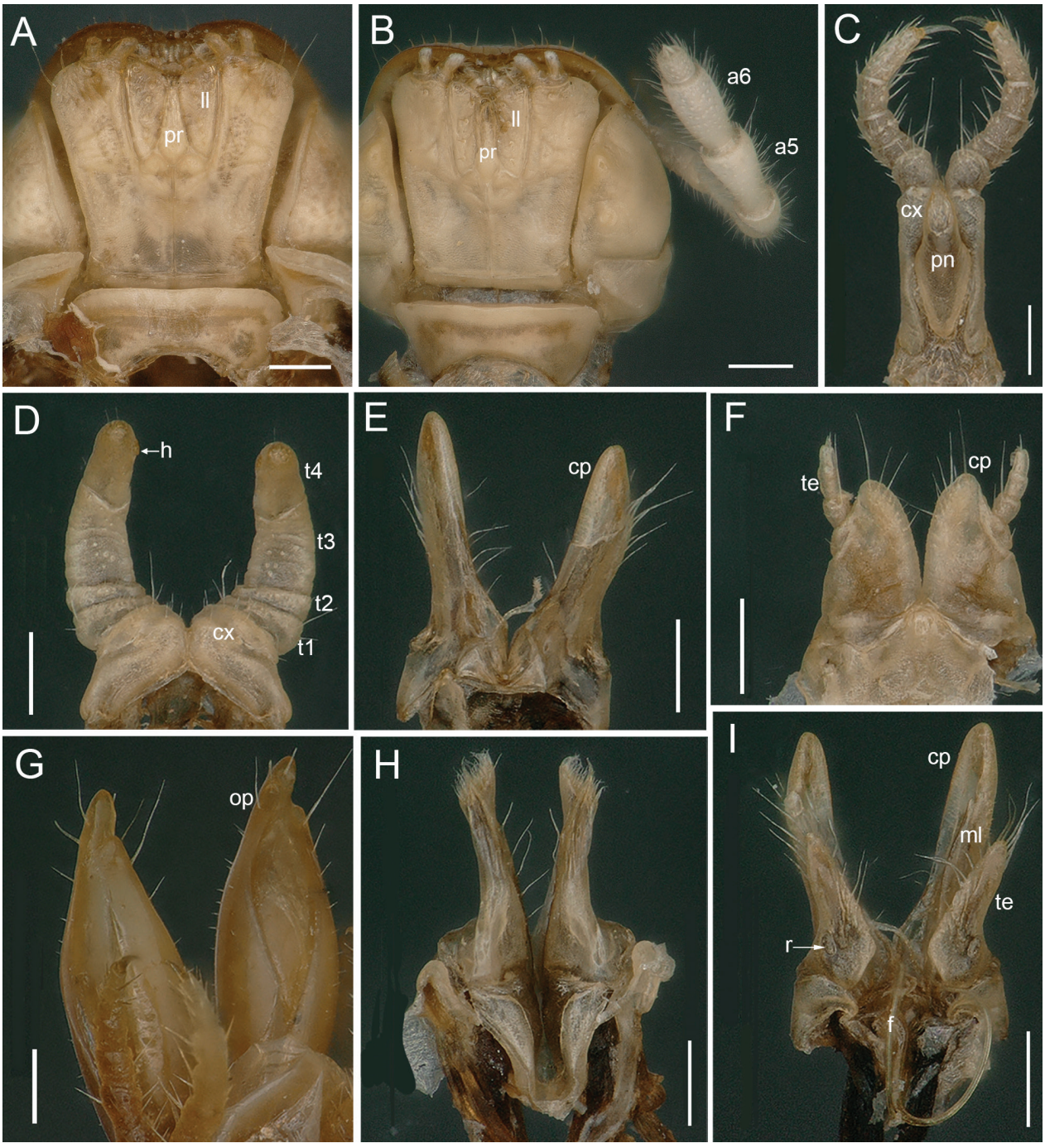

Figure 13. *Skleroprotopus incisodentatus* **sp. nov.**. paratypes from Cave Lingjiu Dong. **A**, **G** female paratype; **B**–**I** male paratype. **A**, **B** gnathochilarium; **C** legs 2 with penis, posterior view; **D** legs 1, anterior view; **E** anterior gonopods, anterior view; **F** legs 7, anterior view; **G** vulvae, lateral view; **H** posterior gonopods, anterior view; **I** anterior gonopods, posterior view. **Abbreviations:** a5, a6, antennomeres 5, 6; cp, coxal process; cx, coxa; f, flagellum; h, hump; ll, lamella lingualis; ml, membranous lobe; op, operculum; pn, penis; pr, promentum; r, remnant; t1–t4, telopoditomeres 1–4; te, telopodite. **Scale bars:** 0.2 mm.

Collum with 11–14 lower striae laterally, but lowest 2 striae not reaching the anterior margin. Prozona with 2–3 irregular subtransverse striae and metazona with 16–25 longitudinal striae laterally. Suture dividing pro- and metazona very narrow, a regular comb. Ozopores starting with ring 6, lying mid-laterally on sides of metatergites.

Epiproct slightly protruding caudad, with 3+3 setae laterally. Paraprocts convex, with 1+1 setae. Hypoproct eye-shaped, with 1+1 setae.

Legs medium-sized, about as long as midbody height. Male leg-pair 1 (Fig. 13D) hypertrophied, 5-segmented, strongly curved anteriad; coxa (**cx**) and telopoditomeres 1 and 2 (**t1**, **t2**) with some scattered long setae. Telopoditomere 3 (**t3**) longest, about 1.5× as long as telopoditomere 4 (**t4**), **t4** irregularly shaped, subapically with a small mesal hump (**h**). Male leg-pair 2 (Fig. 13C) reduced in size; penis (**pn**) relatively thick, only slightly higher than coxae (**cx**), distal part with 3 long setae. Male leg-pair 7 (Fig. 13F) reduced, each leg with a 4-segmented

telopodite (**te**) and a claw, telopoditomere 2 (**t2**) with a long seta subapically; coxal process (**cp**) small, median margin setose.

Anterior gonopods (Fig. 13E, I) with a very long coxal process (**cp**), bearing several short villi laterally, posteriorly carrying with a narrow, lower, membranous lobe (**ml**), outer margin of **ml** smooth, with a vague indentation distally. Flagellum (**f**) very long and slender, distally branched and villose. Telopodite (**te**) about 3/4 as long as **cp**, with long setae both apically and mesally, laterobasally with a minute remnant (**r**) of a second podomere.

Posterior gonopods (Fig. 13H) branched distally, anterior branch smooth, with a pointed tip, posterior one densely setose.

Vulvae (Fig. 13G) as usual, with two parallel rows of short setae on anterior and posterior surfaces, operculum (**op**) with several long setae distally.

Remarks. This species was collected from two caves in the same county in Jiangxi Province, about 6 km apart. However, both are only about 40–50 km away from the collection site/cave in Zhejiang Province. Based on the pigmented body, black eyes, as well as moderately long legs, *S. incisodentatus* **sp. nov.** is considered a troglophile.

3.3.11. *Skleroprotopus multistriatus* sp. nov.

https://zoobank.org/BA22EE32-8DDC-4E15-8B73-59A49D7C9E17

Figures 3G, 14

Material examined. Holotype male (SCAU), China, Zhejiang Province, Hangzhou City, Jiande City, Cave Shenxian Dong, 29°23′27.83″N 119°5′41.26″E, 150 m, 27.XII.2018, Tian Mingyi, Cheng Jingli, Qin Zhuanghui and Chen Mengzhen leg. Paratypes: 22 males, 12 females (SCAU), same data as for holotype.

Diagnosis. Differs from congeners mostly based on the following combination of characters: (1) collum with 10–16 lower striae and 18–27 longitudinal striae laterally on metazona (Fig. 3G). (2) telopoditomere 4 of male leg-pair 1 with two small mesal humps (Fig. 14D); (3) penis stout, distally sharpened, much shorter than coxae 2 (Fig. 14C); (4) male leg 7 with a very small coxal process, only slightly higher than 2-segmented telopodite (Fig. 14E); (5) anterior gonopod (Fig. 14G, H) with a very long and slender coxal process carrying a narrow, lower, membranous lobe, distally with a vague indentation. — In addition, this new species differs from all other *Skleroprotopus* species analyzed in uncorrected *p*-distances ranging from between 8.0–8.3% (compared to *S. incisodentatus* **sp. nov.**) and 14.6% (compared to *S. longissimus* **sp. nov.**).

Etymology. The species is named after the more numerous striae on the collum and metazona; adjective.

Description. Length of males ca 29.5–34.5 mm, 1.8–2.0 mm in diameter, body with 53–59 podous + 1 apodous rings + telson. Length of females ca 34.0–37.0 mm, 1.9–2.1 mm in diameter, body with 57–62 podous + 1–2 apodous rings + telson. Coloration in alcohol (Fig. 3G) generally marbled dark brownish, antennae and legs light brownish. Eye patches blackish, subtriangular, arranged in 4–6 irregular rows, altogether about 26–36 ommatidia per eye patch.

Head capsule smooth and hairless, eyes slightly bulged, epicranial suture well-defined. Labral margin with 2+2 supra-labral and 9+9 labral setae. Antennae long and slender, reaching behind to middle of ring 4 when stretched dorsally. In length, antennomeres 3>2>5>4>6>7>1 (Fig. 14F). Antennomeres 5 and 6 (Fig. 14F) each with a distal corolla of sensilla basiconica. Mandibular stipes well-rounded in male, even more strongly rounded in female. Gnathochilarium with at least 5 setae on each lamella lingualis (**ll**); prementum (**pr**) lute-shaped, anteriorly swollen and very narrow in males (Fig. 14B), vs a narrow, oblong and rhomboid **pr** in females (Fig. 14A).

Collum with 10–16 lower striae laterally, but lowest 4 striae not reaching the anterior margin. Prozona with 2–6 irregular subtransverse striae and metazona with 18–27 longitudinal striae laterally (Fig. 3G). Suture dividing pro- and metazona very narrow, a regular comb. Ozopores starting with ring 6, lying mid-laterally on sides of metatergites.

Epiproct slightly protruding caudad, posterior margin with 4+4 setae. Paraprocts convex, with 1+1 setae. Hypoproct eye-shaped, with 1+1 setae.

Legs medium-sized, about as long as midbody height. Male leg-pair 1 (Fig. 14D) hypertrophied, 5-segmented, strongly curved anteriad; Coxa (**cx**) and telopoditomeres 1 and 2 (**t1**, **t2**) with some scattered long setae. Telopoditomere 3 (**t3**) longest, about 1.5× as long as telopoditomere 4 (**t4**), **t4** irregularly shaped, caudally densely setose, subapically with two small mesal humps (**h**). Male leg-pair 2 (Fig. 14C) reduced in size and somewhat stout; coxae (**cx**) elongated, penis (**pn**) very stout, much shorter than **cx**, distal part sharpened, seta absent. Male leg-pair 7 (Fig. 14E) strongly reduced, each leg with a 2-segmented asymmetrical telopodite (**te**), telopoditomere 1 (**t1**) with several long setae; coxal process (**cp**) very small, slightly higher than **te**, medial margin and distally densely setose.

Anterior gonopods (Fig. 14G, H) with a very long and narrow coxal process (**cp**) bearing a row of short villi in anterior view, posteriorly carrying with a low, narrow, membranous lobe (**ml**), outer margin of **ml** smooth, with a vague indentation distally. Flagellum (**f**) very long and slender, distally branched and villose. Telopodite (**te**) about 2/3 as long as **cp**, with long setae at mesal margin and apically, laterobasally with a minute remnant (**r**) a second podomere.

Posterior gonopods (Fig. 14I) erect, branched distally, anterior branch smooth, with a very small and pointed tip, posterior one densely setose.

Vulva (Fig. 14J) as usual, with two parallel rows of short setae on both anterior and posterior surfaces; operculum (**op**) with 3 long distal setae.

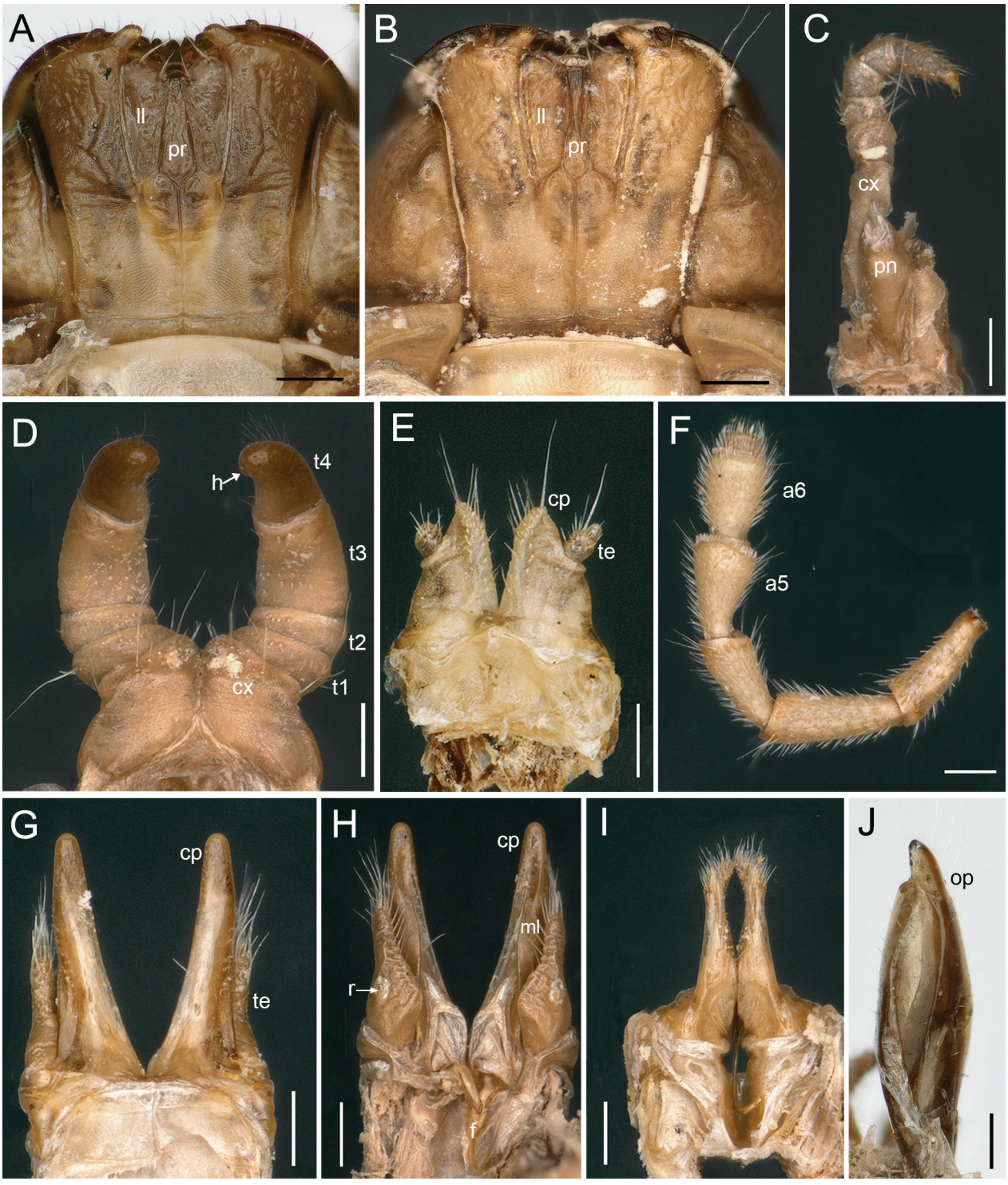

Figure 14. *Skleroprotopus multistriatus* **sp. nov.**. **A**, **J** female paratype; **B**–**I** male paratype. **A**, **B** gnathochilarium; **C** leg 2 with penis, posterior view; **D** legs 1, anterior view; **E** legs 7, anterior view; **F** right antenna, lateral view; **G** anterior gonopods, anterior view; **H** anterior gonopods, posterior view; **I** posterior gonopods, anterior view; **J** right vulva, mesal view. **Abbreviations:** a5, a6, antennomeres 5, 6; cp, coxal process; cx, coxa; f, flagellum; h, hump; ll, lamella lingualis; ml, membranous lobe; op, operculum; pn, penis; pr, promentum; r, remnant; t1–t4, telopoditomeres 1–4; te, telopodite. **Scale bars:** 0.2 mm.

Remarks. Based on the pigmented body, black eyes, as well as moderately long legs, *S. multistriatus* **sp. nov.** is rather to be considered as a troglophile.

3.3.12. *Skleroprotopus conicus* sp. nov.

https://zoobank.org/6EA83681-BB51-45EE-A40B-6B6DE-E144CD4

Figures 3E, 15

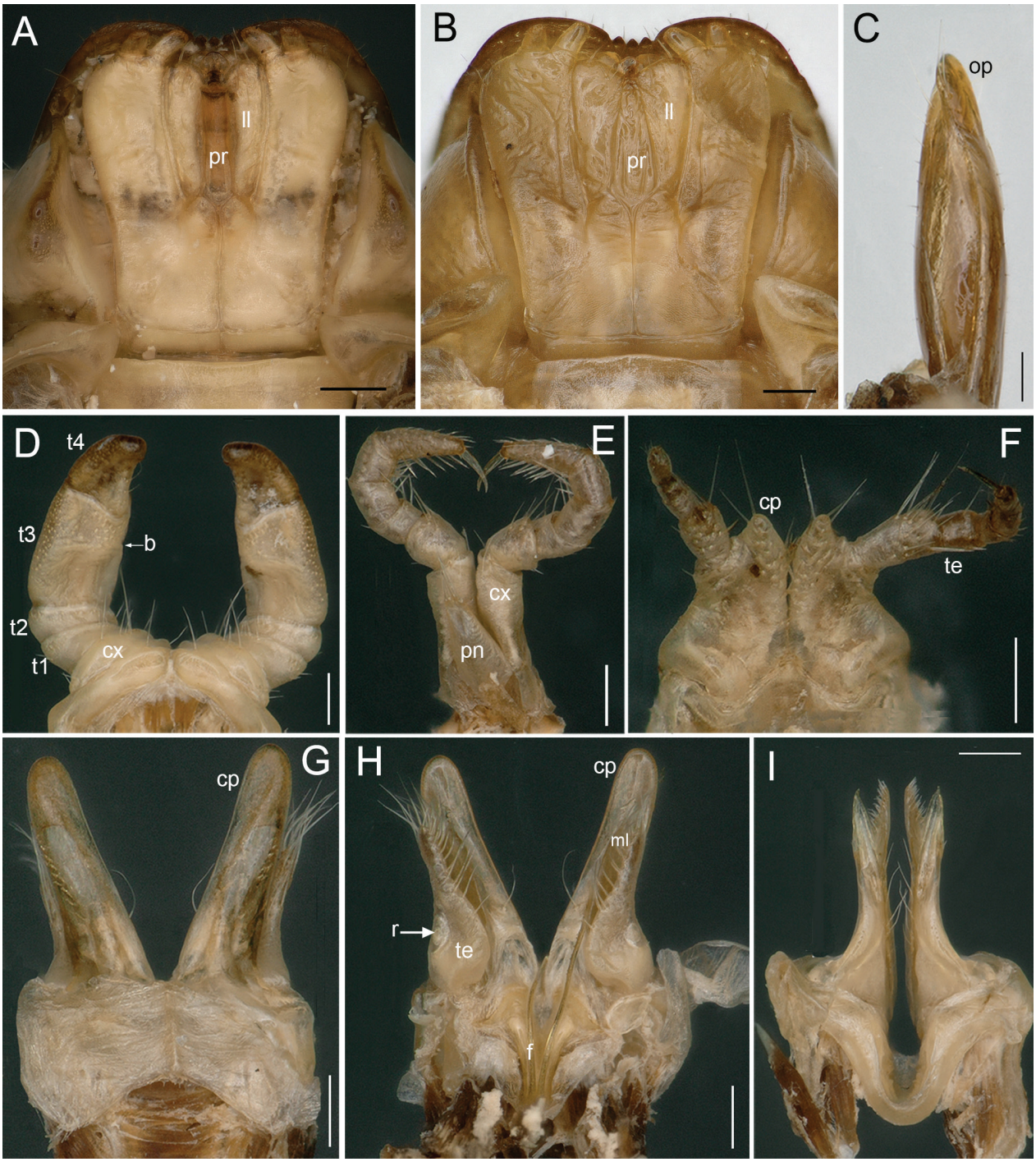

Figure 15. *Skleroprotopus conicus* **sp. nov.**. paratypes from Cave Xianpu Dong. **A, D-I** male paratype; **B**, **C** female paratype. **A**, **B** gnathochilarium; **C** right vulva, mesal view; **D** legs 1, anterior view; **E** legs 2 with penis, posterior view; **F** legs 7, anterior view; **G** anterior gonopods, anterior view; **H** anterior gonopods, posterior view; **I** posterior gonopods, anterior view. **Abbreviations:** b, bulge; cp, coxal process; cx, coxa; f, flagellum; ll, lamella lingualis; ml, membranous lobe; op, operculum; pn, penis; pr, prementum; r, remnant; t1–t4, telopoditomeres 1–4; te, telopodite. **Scale bars:** 0.2 mm.

Material examined. Holotype male (SCAU), China, Zhejiang Province, Jinhua City, Wucheng District, Cave Xianpu Dong, 29°12′23.04″N 119°38′5.47″E, 650 m, 28.XII.2018, Tian Mingyi, Cheng Jingli, Qin Zhuanghui and Chen Mengzhen leg. Paratypes: 8 males, 5 females (SCAU), same data as for holotype; 24 males, 34 females (SCAU), China, Zhejiang Province, Jinhua City, Lanxi City, Cave Baiyun Dong, 29°12′50.19″N 119°32′28.62″E, 300 m, 28.XII.2018, Tian Mingyi, Cheng Jingli, Qin Zhuanghui and Chen Mengzhen leg.

Diagnosis. Differs from congeners mostly based on the following combination of characters: (1) telopoditomere 3 of male leg 1 longest, with a faint bulge in the middle (Fig. 15D); (2) penis very flat, much shorter than coxae 2 (Fig. 15E); (3) male leg 7 with a very small, cone-shaped coxal process and a basically normal telopodite (Fig. 15F); (4) anterior gonopod (Fig. 15G, H) with a very long coxal process carrying a narrow membranous lobe,

outer margin distinctly serrate distally. — In addition, this new species differs from all other species analyzed in a >10.0% uncorrected *p*-distance of the COI barcoding gene.

Etymology. The specific epithet refers to the male leg 7 with a rather small and cone-shaped coxal process; adjective.

Description. Length of both sexes ca 27.0–47.5 mm, width 1.8–2.0 mm in diameter, body with 55–68 podous + 1 apodous ring + telson. Coloration in alcohol uniformly brownish (Fig. 3E), prozona slightly red or dark brownish. Antennae and legs yellowish to light brown. Eye patches blackish, subtriangular, arranged in 6–14 irregular rows, altogether about 32–78 ommatidia per eye patch.

Head capsule smooth and hairless, vertex bulged, epicranial suture clearly concave. Labral margin with 2+2 supra-labral and 7+7 labral setae. Antennae long and slender, reaching behind to middle of ring 4 when stretched dorsally. In length, antennomeres 3>4>5>2≈6>7>1. Antennomeres 5 and 6 each with a distal corolla of sensilla basiconica. Mandibular stipes well-rounded, with two small lobes in males, rounded in females. Gnathochilarium with at least 3 setae on each lamella lingualis (**ll**); prementum (**pr**) short and lanceolate, swollen anteriorly, tube-shaped in males (Fig. 15A), vs an oblong rhomboid **pr** in females (Fig. 15B).

Collum (Fig. 3E) with 5–7 lower striae laterally, but lowest 2 striae not reaching the anterior margin. Prozona with at least 10 irregularly scattered striae and metazona with 13–18 longitudinal striae laterally (Fig. 3E). Suture dividing pro- and metazona very narrow, a regular comb. Ozopores starting with ring 6, lying anteriorly on lateral sides of metatergites.

Epiproct slightly protruding caudad, posterior margin with 2+2 setae. Paraprocts convex, medially with 1+1 setae. Hypoproct eye-shaped, with 1+1 setae.

Legs medium-sized, about as long as midbody height. Male leg-pair 1 (Fig. 15D) hypertrophied, 5-segmented, strongly curved anteriad; coxa (**cx**) and telopoditomeres 1 and 2 (**t1**, **t2**) with some long setae. Telopoditomere 3 (**t3**) longest, with a faint bulge (**b**) in the middle. Telopoditomere 4 (**t4**) irregularly shaped, with few setae medially. Male leg-pair 2 (Fig. 15E) reduced in size and stout; penis (**pn**) very flat, much shorter than coxae (**cx**), distal part with 6 long setae. Male leg-pair 7 (Fig. 15F) with a 4- or 5-segmented telopodite (**te**) sometimes asymmetrical (not including claw); coxal process (**cp**) rather small, cone-shaped, with few long setae apically.

Anterior gonopods (Fig. 15G, H) with a very long coxal process (**cp**) bearing a row of short villi in anterior view, posteriorly carrying with a narrow membranous lobe (**ml**), distal outer margin of **ml** distinctly serrate. Flagellum (**f**) very long and slender, with spikes at margin. Telopodite (**te**) about 3/4 as long as **cp**, with long setae both apically and mesally, laterobasally with a minute remnant (**r**) of a second podomere.

Posterior gonopods (Fig. 15I) erect, branched distally, anterior branch smooth, with a pointed tip, posterior one densely setose.

Vulva (Fig. 15C) as usual, with two parallel rows of short setae on anterior and posterior surfaces; operculum (**op**) with 2 long distal setae.

Remarks. This species was collected from two caves in the same city, about 9 km apart. Based on the pigmented body, black eyes, as well as moderately long legs, *S. conicus* **sp. nov.** is rather to be considered as a troglophile.

3.3.13. *Skleroprotopus laiyuanensis* sp. nov.

https://zoobank.org/DE0C2C91-8D64-4FB8-8351-CBACAE85BECB

Figures 2F, 16

Material examined. Holotype male (SCAU), China, Fujian Province, Longyan City, Liancheng County, Laiyuan Town, Cave Chuqi Dong, 25°33′20″N 116°59′51″E, 950 m, 30.IV.2018, Tian Mingyi and Cheng Jingli leg. Paratypes: 7 males, 11 females (SCAU), same data as for holotype; 2 males, 11 females (SCAU), same location, Cave Shiyan Dong, 29.IV.2018; 3 males, 4 females (SCAU), same location, Cave Yanshang Dong, 30.IV.2018, all Tian Mingyi and Cheng Jingli leg.

Diagnosis. Differs from congeners mostly based on the following combination of characters: (1) telopoditomere 3 of male leg-pair 1 extremely long, longer than all other telopoditomeres combined (Fig. 16D); (2) penis a little longer than coxae 2 (Fig. 16E); (3) male leg-pair 7 with very large coxal processes, about 4× as long as the telopodite (Fig. 16F); (4) anterior gonopod (Fig. 16H, I) with a very long coxal process carrying a narrow, lower, membranous lobe, outer margin distinctly microdentate; and an extremely slender flagellum. — In addition, this new species differs from all other species analyzed in a >10.8% uncorrected *p*-distance of the COI barcoding gene.

Etymology. The species is named after its tye locality within the Laiyuan Karst Cave, which is the largest cave group known in Fujian Province, southeastern China; adjective.

Description. Length of males ca 18.5–35.0 mm, 1.3–1.8 mm in diameter, body with 49–58 podous + 1 apodous rings + telson. Length of females ca 27.0–38.0 mm, 1.8 mm in diameter, body with 53–58 podous + 1 apodous rings + telson. Natural coloration (Fig. 2F) yellowish, in alcohol marbled brownish or red brownish. Antennae and legs yellowish. Eye patches blackish, subtriangular, arranged in 4–6 irregular rows, altogether about 22–43 ommatidia per eye patch.

Head capsule smooth and hairless, eyes slightly bulged, epicranial suture well-defined. Labral margin with 2(3)+2(3) supra-labral and 12+12 labral setae. Antennae very long and slender, reaching behind to middle of ring 5 when stretched dorsally. Antennomeres:

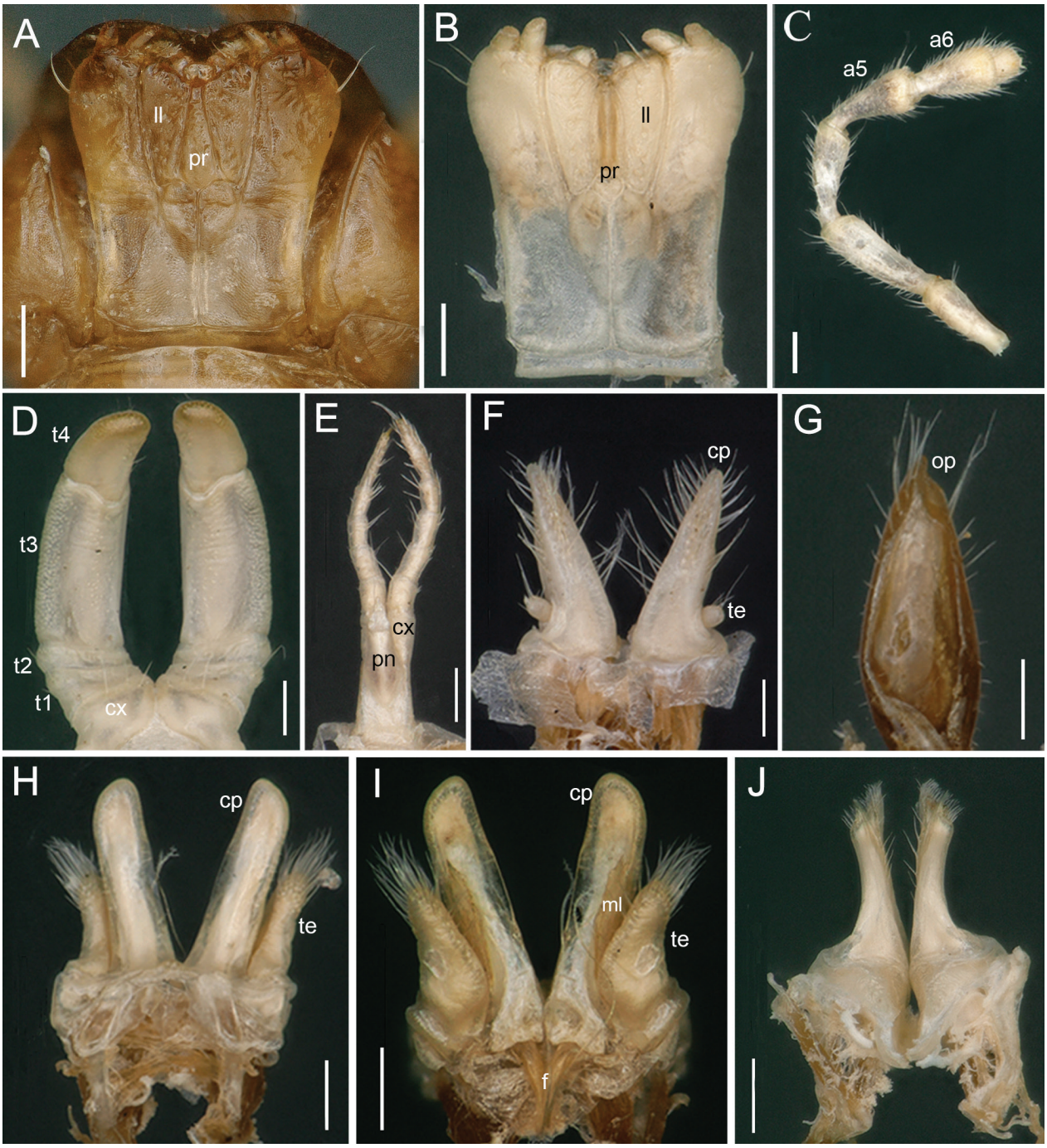

Figure 16. *Skleroprotopus laiyuanensis* **sp. nov.**. paratypes from Cave Chuqi Dong. **A**, **G** female paratype; **B**–**F**, **H**–**J** male paratype. **A**, **B** gnathochilarium; **C** right antenna, lateral view; **D** legs 1, anterior view; **E** legs 2 with penis, posterior view; **F** legs 7, anterior view; **G** left vulva, sublateral view; **H** anterior gonopods, anterior view; **I** anterior gonopods, posterior view; **J** posterior gonopods, anterior view. **Abbreviations:** a5, a6, antennomeres 5, 6; cp, coxal process; cx, coxa; f, flagellum; ll, lamella lingualis; ml, membranous lobe; op, operculum; pn, penis; pr, promentum; t1–t4, telopoditomeres 1–4; te, telopodite. **Scale bars:** 0.2 mm.

3>4>2≈5>6>1>7. Antennomeres 5 and 6 each with a distal corolla of sensilla basiconica (Fig. 16C). Mandibular stipes well-rounded, with two small lobes in males, regularly rounded in females. Gnathochilarium with at least 6 setae on each lamella lingualis (**ll**); promentum (**pr**) heart-shaped at base, the remainder swollen and fusiform in males (Fig. 16B), vs a narrow, oblong and rhomboid **pr** in females (Fig. 16A).

Collum with marbled brownish spots and 11 lower striae laterally, but lowest 2 striae not reaching the anterior margin. Prozona marbled, with 3–4 subtransverse striae and metazona with 20–23 longitudinal striae laterally. Suture dividing pro- and metazona very narrow, a regular comb. Ozopores starting with ring 6, lying mid-laterally on sides of metatergites.

Epiproct slightly protruding caudad, with 7+7 setae at posterior margin. Paraprocts convex, medially with 3+3 setae. Hypoproct eye-shaped, with 1+1 setae.

Legs medium-sized, about as long as midbody height. Male leg-pair 1 (Fig. 16D) hypertrophied, 5-segmented

strongly curved anteriad; coxa (**cx**) and telopoditomeres 1 and 2 (**t1**, **t2**) with several long setae. Telopoditomere 3 (**t3**) longest, longer than all other telopoditomeres combined. Telopoditomere 4 (**t4**) irregularly shaped, medially with a few long setae. Male leg-pair 2 (Fig. 16E) reduced in size and rather slender; penis (**pn**) slightly longer than coxae (**cx**), distal part with three long setae. Male leg-pair 7 (Fig. 16F) strongly modified, with a very small 2-segmented telopodite (**te**), telopoditomere 2 (**t2**) larger, with a few long setae subapically; coxal process (**cp**) about 4.0× as long as **te**, densely setose.

Anterior gonopods (Fig. 16H, I) with a very long coxal process (**cp**) bearing a short row of short villi in anterior view, posteriorly with a narrow and low membranous lobe (**ml**), outer margin of **ml** distinctly microdentate. Flagellum (**f**) very long and extremely slender, distally villose. Telopodite (**te**) about 2/3 as long as **cp**, densely setose apically and mesally.

Posterior gonopods (Fig. 16J) erect and slenderer, distally densely setose; anteriorly with a rather small pointed tip.

Vulva (Fig. 16G) as usual, with two parallel rows of short setae on both anterior and posterior surfaces. Operculum (**op**) subapically with three pairs of long setae, and two long distal setae on bursa.

Remarks. This new species was found in several caves in Laiyuan Karst, which is the largest karst cave group found in eastern China (Fig. 17). Based on the unpigmented body and long antennae, *S. laiyuanensis* **sp. nov.** is rather to be considered as a troglobite.

3.4. A key to Chinese *Skleroprotopus* species (based only on males)

1 Coxal process of leg 7 extremely elongated, much longer than the telopodite (Figs 4E, 9C, 10F, 11F, 16F) **2**
1' Coxal process of leg 7 very short, slightly longer or shorter than the telopodite (Figs 5E, 6D, 7F, 8F, 12E, 13F, 14E, 15F) **8**
2 Coxal process (**cp**) of anterior gonopod with a broad membranous lobe, outer margin clearly exceeding the **cp** (Fig. 4I) **3**
2' Coxal process (**cp**) of anterior gonopod with a narrow membranous lobe, outer margin unexceeding the **cp** (Figs 9H, 10H, 11H, 16I) **4**
3 Eye with blackish ommatidia, epigean species ..... ***S. yutiantianae* sp. nov.**
3' Eye with completely depigmented ommatidia, cave-dwelling species ..... ***S. membranipedalis***
4 Membranous lobe of anterior gonopod coxal process irregularly dentate at outer margin (Figs 10H, 11H, 16I) **5**
4' Membranous lobe of anterior gonopod coxal process with an obvious groove distally (Fig. 9H) ..... ***S. penglai* sp. nov.**
5 Penis slightly longer than coxa 2 (Fig. 16E) ..... ***S. laiyuanensis* sp. nov.**
5' Penis much shorter than coxa 2 (Figs 10E, 11E) **6**
6 Coxal process of leg 7 densely setose throughout at both mesal and lateral margins (Fig. 11F) **7**
6' Coxal process of leg 7 free from setae along distal 2/3 (Fig. 10F) ..... ***S. longissimus* sp. nov.**
7 Telopoditomere 4 of leg 1 with two vague emarginations (Fig. 11D) ..... ***S. genjudi* sp. nov.**
7' Telopoditomere 4 of leg 1 without emargination ..... ***S. serratus***
8 Apex of anterior gonopod coxal process with a protrusion (Figs 16 and 17 in Mikhaljova et al. 2024) ..... ***S. securifer***
8' Apex of anterior gonopod coxal process without a protrusion (Figs 5H, 6I, 7H, 8H, 12I, 13I, 14H, 15H) **9**
9 Posterior gonopods stout (Figs 5F, 6G, J) **10**
9' Posterior gonopods slender (Figs 7I, 8I, 12J, 13H, 14I, 15I) **11**
10 Telopoditomere 3 of leg 1 particularly broad and bulging in the middle (Fig. 6E) ..... ***S. megistus* sp. nov.**
10' Telopoditomere 3 of leg 1 longest, without bulge (Fig. 5D) ..... ***S. tiankeng* sp. nov.**
11 Flagellum distally villose or branched (Figs 7H, 8H, 12I, 13I, 14H, 15H) **12**
11' Flagellum distally simple, smooth ..... ***S. confucius***
12 Flagellum extremely long and slender, higher than the coxal process of anterior gonopod (Fig. 7H) **13**
12' Flagellum very long and slender, while lower than the coxal process of anterior gonopod (Figs 8H, 12I, 13I, 14H, 15H) **14**
13 Coxal process of leg 7 cone-shaped, higher than the telopodite (Fig. 7F) ..... ***S. longiflagellatus* sp. nov.**
13' Coxal process of leg 7 knob-shaped, lower than the telopodite ..... ***S. laticoxalis***
14 Membranous lobe of anterior gonopod coxal process with irregularly dentate at outer margin (Figs 8H, 15H) ... **15**
14' Membranous lobe of anterior gonopod coxal process with an obvious groove distally (Figs 12I, 13I, 14H) … **16**
15 Telopoditomere 3 of leg 1 with a faint bulge in the middle; telopoditomere 4 irregularly shaped, gradually tapering distally (Fig. 15D) ..... ***S. conicus* sp. nov.**
15' Telopoditomere 3 of leg 1 without bulge; telopoditomere 4 rounded distally, with a small mesal hump (Fig. 8E) ..... ***S. change* sp. nov.**
16 Collum and metazona usually with more numerous striae (Fig. 3G) **17**
16' Collum and metazona usually with less numerous striae (Fig. 3D) ..... ***S. ampullaceus* sp. nov.**

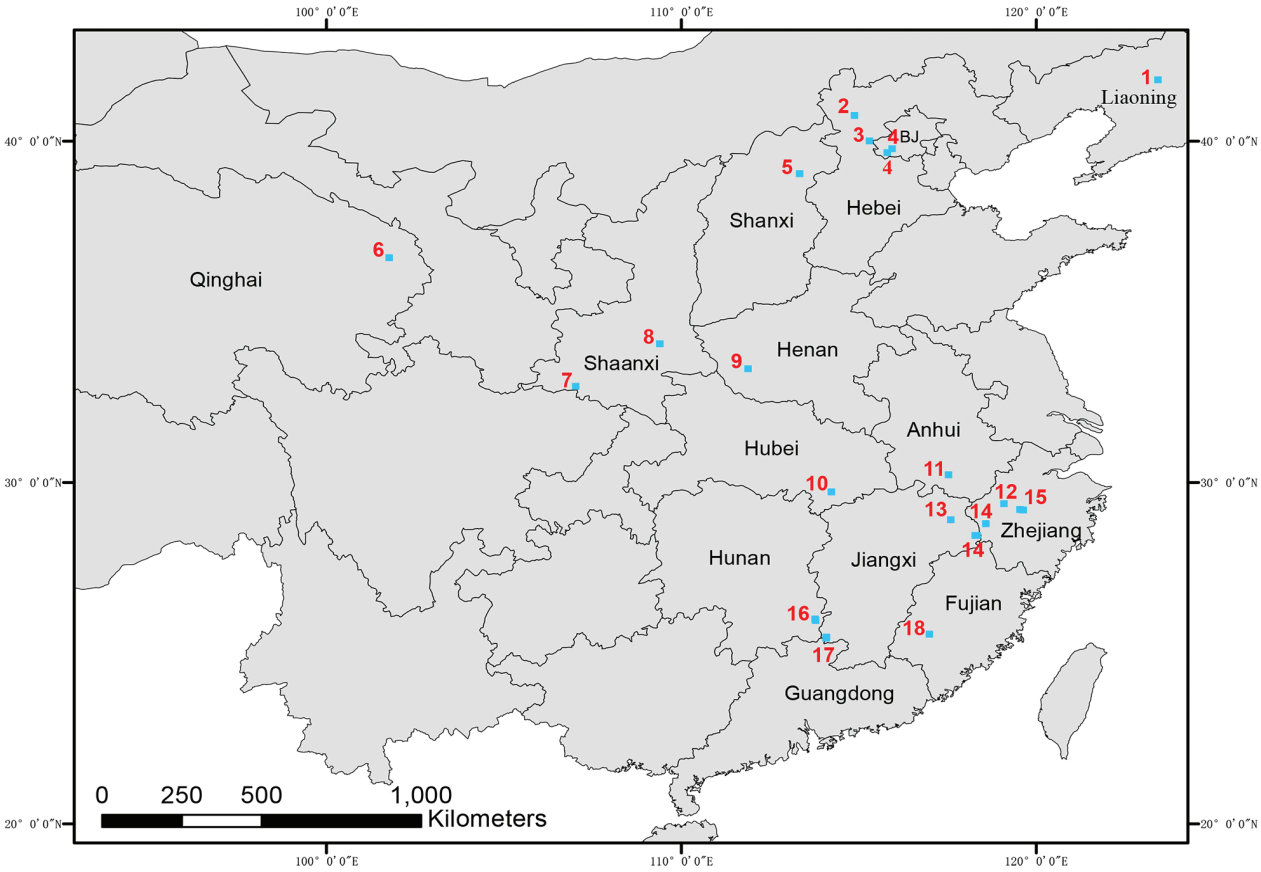

Figure 17. A distribution map of the genus *Skleroprotopus* species in China. **1** *Skleroprotopus laticoxalis*; **2** *S. confucius*; **3** *S. securifer*; **4** *S. membranipedalis*; **5** *S. serratus*; **6** *S. yutiantianae* **sp. nov.**; **7** *S. tiankeng* **sp. nov.**; **8** *S. megistus* **sp. nov.**; **9** *S. longiflagellatus* **sp. nov.**; **10** *S. change* **sp. nov.**; **11** *S. penglai* **sp. nov.**; **12** *S. multistriatus* **sp. nov.**; **13** *S. ampullaceus* **sp. nov.**; **14** *S. incisodentatus* **sp. nov.**; **15** *S. conicus* **sp. nov.**; **16** *S. longissimus* **sp. nov.**; **17** *S. genjudi* **sp. nov.**; **18** *S. laiyuanensis* **sp. nov.** **Abbreviations:** BJ, Beijing.

17 Promentum short and lanceolate, anteriorly swollen (Fig. 13B); penis slightly longer than coxae 2 (Fig. 13C)..... .....***S. incisodentatus* sp. nov.**

17' Promentum lute-shaped, anteriorly swollen and very narrow (Fig. 14B); penis much shorter than coxae 2 (Fig. 14C).....***S. multistriatus* sp. nov.**

4. Discussion

4.1. *Skleroprotopus* species diversity and ecological distribution

In the present study, we combine methods of morphology, molecular phylogenetics, and species delimitation to analyze most species of the millipede family Mongoliulidae recorded from China for the first time. However, three species of the genus *Skleroprotopus* (*S. confucius*, *S. laticoxalis* and *S. serratus*) were not included in the analysis due to lack of samples. The results describe 13 new species, which proves the rich species diversity of *Skleroprotopus* and fills in the research gap of nearly 40 years for this genus in China (Zhang 1985; Vagalinski et al. 2018).

The recognized *Skleroprotopus* species are primarily distributed in the eastern Palearctic, being confined to the Russian Far East, Korea, Japan, and northern China (Enghoff et al. 2017). This distribution pattern seems to indicate that the genus may well represent a group particularly well adapted to temperate climates. Among the 13 new species recorded across nine provinces in China herein (Fig. 17), 12 were collected in caves. Some of these species apparently extend into the Oriental Region. This may be related to our long-term focus on collecting cave-dwelling millipedes, while neglecting the collection of epigean fauna. Additionally, the deep interior of karst caves is relatively constant and usually supports lower mean temperatures compared to the surface environment (Šebela and Turk 2011; Lauritzen 2018). This cooler climate may provide a favorable living environment for the survival of *Skleroprotopus* species, also allowing them to expand further into tropical regions.

In addition, the genus *Glyphiulus* Gervais, 1847 (Spirostreptida, Cambalopsidae) is well known to be among the most common millipede groups in South China Karst

(Golovatch and Liu 2020; Zhao et al. 2022). After extensive surveys of cave millipede faunas, we speculate that ecological niche competition (e.g. O'Neill 1967; Geoffroy 1981; David 2015) may exist between *Glyphiulus* spp. and *Skleroprotopus* spp., representatives of two different families and orders. Currently, there have been no reports of species from both genera living together in the same cave. Such a distribution pattern allows us to speculate about an effective prevention of competition for the limited food resources and environment within the cave. This may be due to the clear-cut preponderance of *Glyphiulus* species to dwelling in and feeding on bat guano (Deharveng and Bedos 2012). In contrast, cavernicolous *Skleroprotopus* species seem to be characteristic, at least mostly if not always, of karst deficient caves or those free from bat guano.

4.2. Taxonomic status issues among species of Mongoliulidae and *Skleroprotopus*

Previous taxonomic studies on the Mongoliulidae primarily used traditional morphological characteristics, often based on the structure of male leg-pair 1, leg-pair 7 and gonopods. Due to the potential lack of significant morphological differences or because some species appear to be quite variable in morphology (Mikhaljova 1997; Mikhaljova and Korsós 2003), this may have led to the creation of numerous synonyms. For instance, *Mongoliulus* Pocock, 1903, *Paraprotopus* Verhoeff, 1939, *Nesoprotopus* Verhoeff, 1939, *Ansiulus* Takakuwa, 1940 and *Senbutudoiulus* Miyosi, 1957 are considered synonyms of *Skleroprotopus* Attems, 1901 (Mikhaljova 2019; Vagalinski et al. 2018). Moreover, significant variations have also been revealed between individuals of different stadia during the postembryonic development (Mikhaljova 2019). This has led to as many as five synonyms listed under *S. coreanus* (Pocock, 1895) alone, a congener particularly widespread both in the Russian Far East and Korea (Mikhaljova 2019). Therefore, the specimens used for descriptions in this study were identified as adult individuals, primarily determined by having only 1 or 2 apodous body rings before the telson and the characteristics of the anterior and posterior gonopods, with further assistance from molecular species delimitation methods to ensure the accuracy of the results.

4.3. Morphological and molecular taxonomy of *Skleroprotopus* species

The ML phylogenetic analyses show that the species of *Skleroprotopus* can be divided into two clades (Fig. 1), one of which contains *S. membranipedalis*, *S. tiankeng* **sp. nov.**, *S. megistus* **sp. nov.** and *S. yutiantianae* **sp. nov.** (clade 1), while the other clade includes *S. penglai* **sp. nov.**, *S. longissimus* **sp. nov.**, *S. conicus* **sp. nov.**, *S. longiflagellatus* **sp. nov.**, *S. change* **sp. nov.**, *S. laiyuanensis* **sp. nov.**, *S. genjudi* **sp. nov.**, *S. ampullaceus* **sp. nov.**, *S. multistriatus* **sp. nov.** and *S. incisodentatus* **sp. nov.** (clade 2). Morphologically, the results support division into the same two groups, mainly because clade 1 has a rather broadened and high membranous lobe on the coxal process of their anterior gonopods (Figs 4I, 5H, 6I) (Zhang 1985). However, *S. penglai* **sp. nov.** is also grouped within this clade in the BI phylogenetic analyses (Fig. S1), but overall, the supports are both relatively weak. Yet the pattern cannot be considered very reliable based on such a limited number of samples.

In addition, we have also summarized other morphological characteristics, but no very clear basis for division was found. For instance, all species of *Skleroprotopus* in China have a male leg-pair 1 composed of 5 segments (coxae + 4-segmented telopodites), with the exception of *S. yutiantianae* **sp. nov.** and *S. membranipedalis* (see Vagalinski et al. 2018, while the original description indicates that male leg-pair 1 consisted of 5 segments, see Zhang 1985), which is composed of a 6-segmented leg-pair 1. In terms of penis length, there are nine species with a penis shorter than the coxae (Figs 4F, 7E, 9F, 10E, 11E, 12F, 14C, 15E) (Vagalinski et al. 2018), vs five species with a penis length equal to or longer than the coxae (Figs 5I, 6F, 8D, 13C, 16E). The length of the penis observed here does not appear to be directly related to the maturity of the specimens. Regarding male leg-pair 7, it can be roughly divided into two types. The first type is represented by extremely well-developed coxal processes, which are much longer than the telopodite (Figs 4E, 9C, 10F, 11F, 16F). The second type includes the species with knob-shaped or cone-shaped, very poorly-developed coxal processes. This type can be further divided into subtypes with coxal processes either slightly longer (Figs 7F, 12E, 14E) or shorter than the telopodite (Figs 5E, 6D, 8F, 13F, 15F).

COI barcoding is the most widely used technique in Animalia to distinguish different taxa due to its universality and high resolution (Hebert et al. 2003). In this study, both COI and 16S were used with two different methods for species delimitation, both yielding consistent results and with all taxonomic units being well delineated. However, during the calculation process, the phylogenetic tree established by 16S was found to be basically consistent with the tree of four genes. In contrast, there were many differences in the ML and BI obtained by COI. This may indirectly reflect the high diversity of *Skleroprotopus* species and a large number of further new species yet to be discovered.

4.4. Adaptation to cave environments

Cave animals are commonly classified into three categories based on their degree of adaptation to the cave environment: troglobites, troglophiles, and trogloxenes (Sket 2008; Howarth and Moldovan 2018; Culver and Pipan 2019). The present study describes 12 new cave-dwelling species and classifies their cave adaptability mainly based on the troglomorphic features exhibited in their external morphology, such as the degeneration of eyes,

unpigmented bodies and the development of legs (Liu et al. 2017). In addition to morphological adaptations, there must be an enhanced focus on studying their habits, behaviors, and ecological adaptations. Future studies should integrate methods such as transcriptomics and genomics to further enhance the understanding of the origins, evolution, and adaptations of cave-dwelling millipedes.

5. Conclusion

The millipede genus *Skleroprotopus* was previously only known to have five species in China, primarily distributed in the northern regions. Through extensive surveys and specimen collection, we have obtained a large number of samples from this group. By utilizing multi-gene molecular data and comparative observations of external morphological characteristics, we discovered 13 new species of the *Skleroprotopus* genus distributed across nine provinces in China. For the first time, we also used barcode analysis to determine their genetic distances. The results of this study greatly enhance our understanding of the species diversity within this genus and provide foundational data for future in-depth analysis of the phylogenetic relationships within the family Mongoliulidae.

6. Declarations

Authors' contributions. RC and YZ have contributed equally to this work.

Conflict of interest. The authors declare that there is no conflict of interest.

Data availability. Sequence information generated in this study is available in NCBI, under accession numbers PQ246765–PQ246783 (COI), PQ282224-PQ282240 (16S), PQ238324–PQ328342 (18S) and PQ238306–PQ238323 (28S).

7. Acknowledgements

The authors wish to express their sincere gratitude to the caving team of the South China Agricultural University, Guangzhou, China, for their collections and support in the field. We are very grateful to Dr. Elena V. Mikhaljova of the Far Eastern Branch of the Russian Academy of Sciences, Vladivostok, Russia, for her suggestions and for sharing her manuscript in the proofreading stage. Special thanks are due to Dr. Dragan Ž. Antić and Dr. Jackson Means for their thorough reviews of the manuscript. This project was supported by the National Natural Science Foundation of China (Grant no. 31801956).

8. References

Altschul SF, Madden TL, Schäffer AA, Zhang J, Zhang Z, Miller W, Lipman DJ (1997) Gapped BLAST and PSIBLAST: a new generation of protein database search programs. Nucleic Acids Research 25(17): 3389–3402. https://doi.org/10.1093/nar/25.17.3389

Culver DC, Pipan T (2019) The biology of caves and other subterranean habitats, second edition. Oxford University Press. 272 pp. https://doi.org/10.1093/oso/9780198820765.001.0001

David J-F (2015) Diplopoda – ecology. In: Minelli A. (ed.), Treatise on Zoology – Anatomy, Taxonomy, Biology. The Myriapoda 2(12): 303–327.

Deharveng L, Bedos A (2012) Diversity patterns in the tropics. In: White WB, Culver DC. (eds), Encyclopedia of caves, second edition. Elsevier: Amsterdam, pp. 238–250. https://doi.org/10.1016/j.quaint.2012.12.013

Edgecombe GD, Giribet G, Wheeler WC (2002) Phylogeny of Henicopidae (Chilopoda: Lithobiomorpha): A combined analysis of morphology and five molecular loci. Systematic Entomology 27: 31–64. https://doi.org/10.1046/j.0307-6970.2001.00163.x

Enghoff H, Jensen LM, Mikhaljova EV (2017) A new genus of mongoliulid millipedes from the Far East of Russia, with a list of species in the family (Diplopoda, Julida, Mongoliulidae). European Journal of Taxonomy 326: 1–19. https://doi.org/10.5852/ejt.2017.326

Enghoff H, Petersen G, Seberg O (2011) Phylogenetic relationships in the millipede family Julidae. Cladistics 27(6): 606–616. https://doi.org/10.1111/j.1096-0031.2011.00360.x

Fischer MM, Getis A (2009) Handbook of Applied Spatial Analysis: Software Tools, Methods and Applications. Springer: Heidelberg, Dordrecht, London, New York, 811 pp. https://doi.org/10.1007/978-3-642-03647-7

Folmer O, Black M, Hoeh W, Lutz R, Vrijenhoek R (1994) DNA primers for amplification of mitochondrial cytochrome c oxidase subunit I from diverse metazoan invertebrates. Molecular Marine Biology and Biotechnology 3: 294–299.

Geoffroy J-J (1981) Modalités de la coexistence de deux diplopodes, *Cylindroiulus punctatus* (Leach) et *Cylindroiulus nitidus* (Verhoeff) dans un ecosystème forestier du Bassin Parisien. Acta Oecologica, Oecologia Generalis 2: 227–243.

Golovatch SI, Liu W-X (2020) Diversity, distribution patterns, and fauno-genesis of the millipedes (Diplopoda) of mainland China. ZooKeys 930: 153–198. https://doi.org/10.3897/zookeys.930.47513

Hebert P, Cywinska A, Ball SL, Dewaard J (2003) Biological identification through DNA barcodes. Proceedings of the Royal Society of London B 270: 313–321.

Howarth FG, Moldovan OT (2018) The ecological classification of cave animals and their adaptations. In: Moldovan OT, Kováč Ľ, Halse S (eds), Cave Ecology. Springer International Publishing, Switzerland: Cham, pp. 41–68. https://doi.org/10.1007/978-3-319-98852-8

Jiang X-K, Shear WAB, Ye L-P, Chen H-M, Xie Z-C (2023) Recovery of the family status of Pericambalidae Silvestri, 1909, stat. nov. (Diplopoda: Spirostreptida: Cambalidea), with a revision of the genera and species from China. Invertebrate Systematics 37(1): 78–100. https://doi.org/10.1071/IS22044

Kumar S, Stecher G, Li M, Knyaz C, and Tamura K (2018) MEGA X: Molecular Evolutionary Genetics Analysis across computing platforms. Molecular Biology and Evolution 35: 1547–1549. https://doi.org/10.1093/molbev/msy096

Lauritzen SE (2018) Physiography of the caves. In: Moldovan OT, Kováč Ľ, Halse S (eds) Cave Ecology. Springer International Publishing, Switzerland: Cham, pp. 7–21. https://doi.org/10.1007/978-3-319-98852-8

Liu W-X, Golovatch SI, Wesener T, Tian M-Y (2017) Convergent evolution of unique morphological adaptations to a subterranean environment in cave millipedes (Diplopoda). PLoS One 12(2): e0170717. https://doi.org/10.1371/journal.pone.0170717

Mikhaljova EV (1997) Review of the cavernicolous millipede fauna of the Far East of Russia, with description of a new troglophilic species (Diplopoda). Arthropoda Selecta 5(3–4): 143–149.

Mikhaljova EV (2004) The millipedes (Diplopoda) of the Asian part of Russia. Pensoft Publishers, Sofia, Bulgaria, 292 pp.

Mikhaljova EV (2019) Identities of the millipede genera *Skleroprotopus* Attems, 1901 and *Ansiulus* Takakuwa, 1940 (Diplopoda: Julida: Mongoliulidae), with emphasis on the postembryonic development of *Skleroprotopus coreanus* (Pocock, 1895). Zootaxa 4551(5): 501–529. https://doi.org/10.11646/zootaxa.4551.5.1

Mikhaljova EV, Kazarin VM, Marusik YM (2024) The millipede genus *Skleroprotopus* Attems, 1901 (Diplopoda, Julida, Mongoliulidae) in China, with description of a new species. Zootaxa 5536(3): 483–491. https://doi.org/10.11646/zootaxa.5536.3.8

Mikhaljova EV, Korsós Z (2003) Millipedes (Diplopoda) from Korea, the Russian far east, and China in the collection of the Hungarian Natural History Museum. Acta Zoologica Academiae Scientiarum Hungaricae 49(3): 215–242.

Muraji M, Tachikawa S (2000) Phylogenetic analysis of water striders (Hemiptera: Gerroidea) based on partial sequences of mitochondrial and nuclear ribosomal RNA genes. Entomological Science 3: 615–626. https://api.semanticscholar.org/CorpusID:83444254

O'Neill RV (1967) Niche segregation in seven species of diplopods. Ecology 48: 983.

Šebela S, Turk J (2011) Air temperature characteristics of the Postojna and Predjama cave systems. Acta Geographica Slovenica 51(1): 43–64. https://doi.org/10.3986/AGS51102

Shull VL, Vogler AP, Baker MD, Maddison DR, Hammond PM (2001) Sequence alignment of 18S ribosomal RNA and the basal relationships of adephagan beetles: evidence for monophyly of aquatic families and the placement of Trachypachidae. Systematic Biology 50(6): 945–969. https://doi.org/10.1080/106351501753462894.

Sket B (2008) Can we agree on an ecological classification of subterranean animals? Journal of Natural History 42: 1549–1563.

Simon C, Frati F, Beckenbach A, Crespi B, Liu H, Flook P (1994) Evolution, weighting, and phylogenetic utility of mitochondrial gene sequences and a compilation of conserved polymerase chain reaction primers. Annals of the Entomological Society of America 87: 651–701. https://doi.org/10.1093/aesa/87.6.651

Vagalinski B, Meng K, Bachvarova D, Stoev P (2018) A redescription of the poorly known cave millipede *Skleroprotopus membranipedalis* Zhang, 1985 (Diplopoda, Julida, Mongoliulidae), with an overview of the genus *Skleroprotopus* Attems, 1901. Subterranean Biology 26: 55–66. https://doi.org/10.3897/subtbiol.26.26225

Xiang C, Gao FL, Jakovlić I, Lei H-P, Hu Y, Zhang H, Zou H, Wang G-T, Zhang D (2023) Using PhyloSuite for molecular phylogeny and tree-based analyses. Imeta 2(1): e87. https://doi.org/10.1002/imt2.87

Zhang CZ (1985) A new millipede of the genus *Skleroprotopus* in Stone Buddha Cave, Fangsheng County, Beijing. Karst Geomorphology and Speleology, Science Press, Beijing: 154–156. [In Chinese]

Zhao Y, Guo W-R, Golovatch SI, Liu W-X (2022) Revision of the *javanicus* species group of the millipede genus *Glyphiulus* Gervais, 1847, with descriptions of five new species from China (Diplopoda, Spirostreptida, Cambalopsidae). ZooKeys 1108: 89–118. https://doi.org/10.3897/zookeys.1108.85156

Supplementary Material 1

Table S1

Authors: Chen R, Zhao Y, Golovatch S, Liu W-X (2024)
Data type: .xlsx
Explanation notes: The four gene fragments that were amplified and their primer information.

Link: https://doi.org/10.3897/asp.82.e136751.suppl1

Supplementary Material 2

Table S2

Authors: Chen R, Zhao Y, Golovatch S, Liu W-X (2024)
Data type: .xlsx
Explanation notes: Genetic *p*-distances for the 669 barcoding bp of the COI gene between *Skleroprotopus* and some outgroup taxa.

Link: https://doi.org/10.3897/asp.82.e136751.suppl2

Supplementary Material 3

Figure S1

Authors: Chen R, Zhao Y, Golovatch S, Liu W-X (2024)
Data type: .jpg
Explanation notes: Bayesian consensus tree based on four-gene fragments sequences.

Link: https://doi.org/10.3897/asp.82.e136751.suppl3